Multi-time correlations in the positive-P, Q, and doubled phase-space representations

Piotr Deuar

Institute of Physics, Polish Academy of Sciences, Aleja Lotników 32/46, 02-668 Warsaw, Poland

arXiv:2011.10107v2 [quant-ph] 6 May 2021

A number of physically intuitive results for the calculation of multi-time correlations in phase-space representations of quantum mechanics are obtained. They relate time-dependent stochastic samples to multi-time observables, and rely on the presence of derivative-free operator identities. In particular, expressions for time-ordered normal-ordered observables in the positive-P distribution are derived which replace Heisenberg operators with the bare time-dependent stochastic variables, confirming extension of earlier such results for the Glauber-Sudarshan P. Analogous expressions are found for the anti-normal-ordered case of the doubled phase-space Q representation, along with conversion rules among doubled phase-space s-ordered representations. The latter are then shown to be readily exploited to further calculate anti-normal and mixed-ordered multi-time observables in the positive-P, Wigner, and doubled-Wigner representations. Which mixed-order observables are amenable and which are not is indicated, and explicit tallies are given up to 4th order. Overall, the theory of quantum multi-time observables in phase-space representations is extended, allowing non-perturbative treatment of many cases. The accuracy, usability, and scalability of the results to large systems is demonstrated using stochastic simulations of the unconventional photon blockade system and a related Bose-Hubbard chain. In addition, a robust but simple algorithm for integration of stochastic equations for phase-space samples is provided.

1 Introduction

Phase-space representations of quantum mechanics such as the Wigner, P, positive-P, Q and related approaches are a powerful tool for the study and understanding of quantum mechanics [14, 50, 62, 93, 118]. Their use in recent times has been directed particularly as a tool in quantum information science (see [58] and [129] for recent reviews) and for the simulation of large-scale quantum dynamics. Negativity of Wigner, P, and other phase-space quasi-distributions is a major criterion for quantumness and closely related to contextuality and nonlocality in quantum mechanics [58, 65]. The inability to interpret the Glauber-Sudarshan P [67, 132] and Wigner distributions in terms of a classical probability density is the fundamental benchmark for quantum light [88, 128]. Quasi-probability representations arise naturally when looking for hidden variable descriptions and an ontological model of quantum theory [16, 58, 93, 127]. Wigner and P-distribution negativity are considered a resource for quantum computation [8, 58] and closely related to magic state distillation and quantum advantage [138]; the Glauber-Sudarshan P distribution defines a hierarchy of nonclassicalities and nonclassicality witnesses [88, 139] and can be experimentally reconstructed [3, 83]. Moreover, P, Q and Wigner distributions and have been used for simulations of models important for quantum information topics such as open spin-qubit systems [136] and boson sampling [53, 112, 113].

For simulation of quantum mechanics, the prime advantage of the phase-space approach is that its computational cost typically grows only linearly with system size even in interacting systems of many particles. Therefore it provides a route to the non-perturbative treatment of the quantum dynamics of large systems. It has been used for solving and simulating a multitude of problems in various physical fields: e.g. quantum optics [21, 28, 30, 32, 52, 54, 84, 91, 110], ultracold atoms [22, 39, 40, 49, 74, 82, 94, 95, 101, 102, 108, 125, 131, 134, 144], fermionic systems [6, 7, 27, 29], spin systems [11, 106, 107], nuclear physics [137], dissipative systems in condensed matter [26, 45, 143], or cosmology [111]. The vast majority of such calculations so far have considered only equal time correlations and observables.

Multi-time correlations are also important for answering many physical questions which cannot necessarily be dealt with by monitoring the time dependence of equal time observables [13, 62, 92, 118, 139]. For example, the determination of lifetimes in an equi-

Piotr Deuar: deuar@ifpan.edu.pl

librium or stationary state, response functions, out-of-time-order correlations (OTOCs), or finding the time resolution required to observe a transient phenomenon. However their calculation in the phase-space framework has been restricted because few general results have been available. What is known is largely restricted to time- and normal-ordered correlations in the Glauber-Sudarshan P representation[5, 62], time-symmetric ones in the truncated Wigner representation [13, 115], or the corresponding linear response corrections for closed systems. The Glauber-Sudarshan P representation results provide a particularly intuitive framework, simply replacing Heisenberg operators $\widehat{a}^\dagger(t)$ and $\widehat{a}(t)$ with time-dependent phase-space variables in normal-ordered observables such as $\widehat{a}^\dagger(t_1)\widehat{a}(t_2)$. They also apply to open systems [2, 62]. Such ordering corresponds to general photon counting measurements [67, 68, 81]. Still, while scaling with system size is excellent, both above approaches usually end up being only approximate because one is forced to omit part of the full quantum mechanics in their numerical implementations [62]. Hence, a broader application of full quantum phase-space methods to multi-time observables would be advantageous. This is especially so, since recent years have shown a lot of interest in such quantities, be it in the study of nonclassicality in the time dimension [9, 89, 104, 119], time crystals [55, 135, 142, 145], quantum technologies [78, 96, 103] where time correlations and time resolution are crucial, methods development [86, 115], and the OTOCs that have recently found to be important for the study of quantum scrambling [15, 64, 133], quantum chaos [98, 124] and many-body localisation [56, 70]. Therefore, this paper sets out to extend the infrastructure available for multi-time observables with phase-space methods.

The positive-P representation [50] does not suffer from the limitations of the Glauber-Sudarshan P (seen e.g. in Sec. 7.3) due to its anchoring in doubled phase space. This allows it to incorporate the full quantum mechanics for most Hamiltonians, including all two-body interactions. Importantly, as we shall see, the same applies for its differently ordered analogues like the doubled-Wigner and doubled-Q. While the positive-P is known to be limited to short times for closed systems due to a noise amplification instability [38, 66], this abates in dissipative systems [45, 66]. Recent work has shown that a very broad range of driven dissipative Bose-Hubbard models can be simulated with the positive-P into and beyond the stationary state [45]. This covers systems of current interest such as micropillars, transmon qubits, and includes strong quantum effects such two-photon interference in the unconventional photon blockade [10, 96], making its extension quite timely.

Therefore, after basic background in Sec. 2, the first order of business in this paper in Sec. 3 is to extend the long known Glauber-Sudarshan P results on time- and normal-ordered multi-time correlations to the positive-P representation. This is sort of an obvious extension, but was missing from the literature, and allows complete quantum calculations. It also lets us explain the ins and outs and set the stage for the less obvious and broader extensions that follow:

The first one of those in Sec. 4.1 considers general representations and reformulates the case of Q representations in an operational form that can be extended to doubled phase-space. This gives stochastic access to anti-normal ordered observables such as $\widehat{a}(t_1)\widehat{a}^\dagger(t_2)$. It is then shown in Sec. 5 how the Gaussian convolution relationship between Wigner, P, and Q distributions allows one to easily evaluate anti-normal ordered correlations in Wigner and P. This is extended also to a wide range of mixed ordered observables such as $\widehat{a}^\dagger(t_1)\widehat{a}(t_2)\widehat{a}^\dagger(t_3)\widehat{a}(t_4)$ in Sec. 5.4, and further extended to cover doubled phase-space representations in Sec. 6. In Sec. 7, the use and accuracy of this approach is demonstrated on the numerical example of the unconventional photon blockade, a system that may have application to the creation of single-photon sources. Finally, Appendix A gives details of a robust algorithm for integrating the resulting phase-space stochastic equations, a matter that has been somewhat neglected in the literature to date.

2 Background

2.1 Positive-P representation

Consider an M-mode system (modes $1,\ldots,j,\ldots,M$) with bosonic annihilation operators $\widehat{a}_j$ for the jth mode. The density operator of the system is written in terms of bosonic coherent states of complex amplitude α_j defined relative to the vacuum:

$$|\alpha_j\rangle_j = e^{-|\alpha_j|^2/2}\, e^{\alpha_j \widehat{a}_j^\dagger}|\mathrm{vac}\rangle, \tag{1}$$

using [50]:

$$\widehat{\rho} = \int d^{4M}\boldsymbol{\lambda}\; P_+(\boldsymbol{\lambda})\,\widehat{\Lambda}(\boldsymbol{\lambda}) \tag{2a}$$

$$\widehat{\Lambda}(\boldsymbol{\lambda}) = \bigotimes_j \frac{|\alpha_j\rangle_j\langle\beta_j^*|_j}{\langle\beta_j^*|_j|\alpha_j\rangle_j}. \tag{2b}$$

The kernel $\widehat{\Lambda}$ involves "ket" $|\alpha_j\rangle_j$ and "bra" $\langle\beta_j^*|_j$ states described by separate and independent variables. Let us define the container variable

$$\boldsymbol{\lambda} = \{\alpha_1,\ldots,\alpha_M,\beta_1,\ldots,\beta_M\} = \{\lambda_\mu\} \tag{3}$$

as a shorthand to hold the full configuration information. Individual complex variables λ_μ can be indexed by $\mu = 1, \ldots, 2M$. The *positive-P* distribution P_+ is guaranteed real and non-negative [50]. This is essential for the utility of the method, which lies in its ability to represent full quantum mechanics using stochastic trajectories of the *samples* $\boldsymbol{\lambda}$ of the distribution P_+. Notably, the size of these samples scales merely linearly with M, allowing for the simulation of the full quantum dynamics of systems with even millions of modes [39, 82].

The distribution (2) can be compared to the simpler and more widely known *Glauber-Sudarshan P representation* [67, 132], which uses a single set of coherent state amplitudes and ties the "bra" and "ket" amplitudes to be equal. It is written

$$\widehat{\rho} = \int d^{2M}\boldsymbol{\alpha}\; P(\boldsymbol{\alpha}) \bigotimes_j |\alpha_j\rangle_j\langle\alpha_j|_j, \tag{4}$$

where the multimode coherent amplitude is $\boldsymbol{\alpha} = \{\alpha_1, \ldots, \alpha_M\}$. This representation gives a well behaved representation of only a subset of possible quantum states [20, 128], though a very useful one that includes Gaussian density operators [4].

For full computational utility of the positive-P method, all quantum mechanical actions should be able to be written in terms of the samples $\boldsymbol{\lambda}$. Central to this are the following identities:

$$\widehat{a}_j\widehat{\Lambda} = \alpha_j\widehat{\Lambda}, \tag{5a}$$

$$\widehat{a}_j^\dagger\widehat{\Lambda} = \left[\beta_j + \frac{\partial}{\partial\alpha_j}\right]\widehat{\Lambda}, \tag{5b}$$

$$\widehat{\Lambda}\widehat{a}_j = \left[\alpha_j + \frac{\partial}{\partial\beta_j}\right]\widehat{\Lambda}, \tag{5c}$$

$$\widehat{\Lambda}\widehat{a}_j^\dagger = \beta_j\widehat{\Lambda}. \tag{5d}$$

A general master equation for the density matrix written in Lindblad form with reservoir operators $\widehat{R}_n$ is

$$\frac{\partial\widehat{\rho}}{\partial t} = -\frac{i}{\hbar}\left[\widehat{H}, \widehat{\rho}\right] + \sum_n \left[2\widehat{R}_n\widehat{\rho}\widehat{R}_n^\dagger - \widehat{R}_n^\dagger\widehat{R}_n\widehat{\rho} - \widehat{\rho}\widehat{R}_n^\dagger\widehat{R}_n\right]. \tag{6}$$

This can be transformed by standard methods [62], using identities (5), to a partial differential equation (PDE) for P_+ of the following general form:

$$\frac{\partial P_+}{\partial t} = \left\{\sum_{n=1}^{n_{\max}}\sum_{\mu_1,\ldots,\mu_k}^{2M}\left(\prod_{k=1}^{n}\frac{\partial}{\partial\lambda_{\mu_k}}\right)F_{\mu_1,\ldots,\mu_n}(\boldsymbol{\lambda})\right\}P_+, \tag{7}$$

with maximum differential order $n_{\max}$ and coefficients F that depend on the details of (6). Most cases have $n_{\max} \leqslant 2$, in which case this is a Fokker-Planck equation (FPE):

$$\frac{\partial P_+}{\partial t} = \left\{\sum_\mu \frac{\partial}{\partial\lambda_\mu}\left[-A_\mu(\boldsymbol{\lambda})\right] + \sum_{\mu\nu}\frac{\partial^2}{\partial\lambda_\mu\partial\lambda_\nu}\frac{D_{\mu\nu}(\boldsymbol{\lambda})}{2}\right\}P_+. \tag{8}$$

An exception occurs if irreducible higher order partial derivatives appear, e.g. due to explicit three-body interactions in the Hamiltonian. Most first principles models use only two-particle interactions, though.

Standard methods convert an FPE like (8) to the following Ito stochastic equations of the samples [62]:

$$\frac{d\lambda_\mu}{dt} = A_\mu(\boldsymbol{\lambda}) + \sum_\sigma B_{\mu\sigma}(\boldsymbol{\lambda})\xi_\sigma(t) \tag{9}$$

where

$$D_{\mu\nu} = \sum_\sigma B_{\mu\sigma}B_{\nu\sigma} \tag{10}$$

i.e. $D = BB^T$ in matrix notation, and $\xi_\sigma(t)$ are independent real white noises with variances

$$\langle\xi_\mu(t)\xi_\nu(t')\rangle_{\text{stoch}} = \delta(t-t')\delta_{\mu\nu}. \tag{11}$$

The notation $\langle\cdot\rangle_{\text{stoch}}$ indicates a stochastic average over the samples. The equations (9) give us quantum mechanical evolution in terms of the samples, which becomes ever more exact as the number of samples grows. Quantum expectation values at a given time are evaluated via

$$\langle\widehat{a}_{j_1}^\dagger\cdots\widehat{a}_{j_\mathcal{N}}^\dagger\widehat{a}_{k_1}\cdots\widehat{a}_{k_\mathcal{M}}\rangle = \langle\beta_{j_1}\cdots\beta_{j_\mathcal{N}}\alpha_{k_1}\cdots\alpha_{k_\mathcal{M}}\rangle_{\text{stoch}}. \tag{12}$$

The equivalence can be written more explicitly in terms of $\mathcal{S}$ individual samples $\boldsymbol{\lambda}^{(u)}$ labelled by $u = 1, \ldots, \mathcal{S}$ as:

$$\langle\widehat{a}_{j_1}^\dagger\cdots\widehat{a}_{j_\mathcal{N}}^\dagger\widehat{a}_{k_1}\cdots\widehat{a}_{k_\mathcal{M}}\rangle = \lim_{\mathcal{S}\to\infty}\tfrac{1}{\mathcal{S}}\textstyle\sum_u \beta_{j_1}^{(u)}\cdots\beta_{j_\mathcal{N}}^{(u)}\alpha_{k_1}^{(u)}\cdots\alpha_{k_\mathcal{M}}^{(u)}. \tag{13}$$

The mode labels in the above can be in any combination, provided all annihilation operators are to the right of all creation operators (which is called "normal ordering"). Any single-time operator can be expressed as a sum of normally ordered terms like (12).

2.2 Multi-time averages in open systems

The situation is much more complicated when the operators in the expectation value are not evaluated all at the same time. The root of the difficulty is that multi-time commutation relations usually depend nontrivially on the full system dynamics, and a reduction of arbitrary multi-time operators to a normal-ordered form is not generally possible.

To describe what is meant at the operator level it is first helpful to introduce the two-sided evolution operator $\breve{V}(t_1,t_2)$ such that evolution by the master equation (6) can be summarised as

$$\widehat{\rho}(t_2) = \breve{V}(t_2,t_1)\widehat{\rho}(t_1). \tag{14}$$

Notably, the evolution operator has the semigroup property [130] $\breve{V}(t_3,t_2)\breve{V}(t_2,t_1) = \breve{V}(t_3,t_1)$. We will use the convention that two-sided operators, indicated by a breve $\breve{}$, act on everything to their right. Hence

$$\breve{V}AB = \breve{V}\{AB\} \neq \left\{\breve{V}A\right\}B. \tag{15}$$

Let us also define the *time-ordered form* via

$$\langle \widehat{A}_1(t_1)\widehat{A}_2(t_2)\cdots\widehat{A}_{\mathcal{N}}(t_{\mathcal{N}})\widehat{B}_1(s_1)\widehat{B}_2(s_2)\cdots\widehat{B}_{\mathcal{M}}(s_{\mathcal{M}})\rangle \tag{16}$$

where the $\widehat{A}_j(t)$ and $\widehat{B}_j(t)$ are Heisenberg picture operators, and the times obey

$$t_1 \leqslant t_2 \leqslant \ldots \leqslant t_{\mathcal{N}} \tag{17a}$$

$$s_1 \geqslant s_2 \geqslant \ldots \geqslant s_{\mathcal{M}}. \tag{17b}$$

There are $\mathcal{N}$ operators $\widehat{A}$ with times labelled $t_1,\ldots,t_{\mathcal{N}}$ increasing to the right, inward, and $\mathcal{M}$ operators $\widehat{B}$ with times labelled $s_1,\ldots,s_{\mathcal{M}}$ increasing to the left, also inward. The location of the inner "meeting point" is arbitrary, and the number of $\widehat{A}$ or $\widehat{B}$ operators can also be zero. No particular constraints are imposed on the $\widehat{A}$ and $\widehat{B}$ operators, except that they should be single time quantities. These operators refer to measurements made at the respective times τ_r, when the density operator was $\widehat{\rho}(\tau_r)$. Between measurements the state evolves according to the master equation (6) (i.e. (14)).

It has been shown [62] that multi-time correlations that correspond to sequences of measurements can always be written in the above form (16). Therefore this time ordering is not an arbitrary one, and not particularly restrictive in itself. It has also been shown that a general time-ordered correlation function (16) obeying (17) can be written in a form that uses the $\breve{V}$. To do so it is necessary to be careful about operator ordering. Following [62], let us order all the times t_p and s_q in the correlation in sequence from earliest to latest. Let us then rename them τ_r so that

$$\tau_1 \leqslant \tau_2 \leqslant \cdots \leqslant \tau_{\mathcal{R}-1} \leqslant \tau_{\mathcal{R}} \tag{18}$$

with $\mathcal{R} = \mathcal{N} + \mathcal{M}$. We also define the corresponding two-sided operators $\breve{F}_r$

$$\breve{F}_r\widehat{\rho} = \begin{cases} \widehat{\rho}\widehat{A}_p & \text{if } \tau_r = t_p \\ \widehat{B}_q\widehat{\rho} & \text{if } \tau_r = s_q \end{cases} \tag{19}$$

Then,

$$\begin{aligned}\langle \widehat{A}_1(t_1)\widehat{A}_2(t_2)\cdots\widehat{A}_{\mathcal{N}}(t_{\mathcal{N}})\widehat{B}_1(s_1)\widehat{B}_2(s_2)\cdots\widehat{B}_{\mathcal{M}}(s_{\mathcal{M}})\rangle \\ = \mathrm{Tr}\Big[\breve{F}_{\mathcal{R}}\breve{V}(\tau_{\mathcal{R}},\tau_{\mathcal{R}-1})\breve{F}_{\mathcal{R}-1}\breve{V}(\tau_{\mathcal{R}-1},\tau_{\mathcal{R}-2})\cdots \\ \cdots\breve{F}_2\breve{V}(\tau_2,\tau_1)\breve{F}_1\widehat{\rho}(\tau_1))\Big].\end{aligned} \tag{20}$$

2.3 Multi-time correlations in the Glauber-Sudarshan P representation

Time-ordered correlations for the Glauber-Sudarshan P representation and a range of other single-phase space representations like the Husimi Q were first studied by Agarwal and Wolf in a Greens function framework [1] extended to the case of open systems [2] and for Hamiltonian systems in a formal integral form [5]. Later, Gardiner [62] used a different more operational approach to derive equivalent expressions for normally and time-ordered operator averages in the Glauber-Sudarshan P representation. These have an intuitive form similar to the single-time stochastic expression (12), as follows:

$$\begin{aligned}\langle \widehat{a}^\dagger_{p_1}(t_1)\cdots\widehat{a}^\dagger_{p_{\mathcal{N}}}(t_{\mathcal{N}})\widehat{a}_{q_1}(s_1)\cdots\widehat{a}_{q_{\mathcal{M}}}(s_{\mathcal{M}})\rangle = \\ \langle \alpha^*_{p_1}(t_1)\cdots\alpha^*_{p_{\mathcal{N}}}(t_{\mathcal{N}})\alpha_{q_1}(s_1)\cdots\alpha_{q_{\mathcal{M}}}(s_{\mathcal{M}})\rangle_{\mathrm{stoch}}\end{aligned} \tag{21}$$

provided the times are ordered according to (17). The requirement that the operators in (21) be normally ordered is an additional constraint on top of time-ordering (17), but one that leads to all operators sorted as they occur in photo-counting theory [81]. It covers a very large subset of the potentially physically interesting correlations. The Gardiner approach is more amenable to extension to doubled phase space and will be used in what follows.

This ordering can be contrasted with the *time-symmetric* ordering for which straightforward truncated Wigner correspondences for closed system evolution were found in [13, 115, 118]. Examples of time-symmetric ordered quantities are $\frac{1}{2}\left[\widehat{a}^\dagger(t_2)\widehat{a}(t_1) + \widehat{a}(t_1)\widehat{a}^\dagger(t_2)\right]$ and $\frac{1}{4}\left[\widehat{a}(t_1)\widehat{a}(t_2)\widehat{a}^\dagger(t_3) + \widehat{a}(t_2)\widehat{a}^\dagger(t_3)\widehat{a}(t_1) + \widehat{a}(t_1)\widehat{a}^\dagger(t_3)\widehat{a}(t_2) + \widehat{a}^\dagger(t_3)\widehat{a}(t_2)\widehat{a}(t_1)\right]$.

3 Time ordered moments in the positive-P representation

3.1 Normally ordered observables

To derive an expression like (21) for the *positive*-P representation, we will follow Gardiner's approach [62] that was previously used for the Glauber-Sudarshan P. Smaller steps will, however, be taken here to draw attention to a few subtleties that will be necessary later.

3.1.1 First order correlation function

First consider the correlation

$$G^{(1)}(t',t) = \langle \widehat{a}_j^\dagger(t')\widehat{a}_k(t)\rangle. \tag{22}$$

Comparing to (20), we can identify $\widehat{A}_1 = \widehat{a}_j^\dagger$, $\widehat{B}_1 = \widehat{a}_k$, and the times $t_1 = t'$, $s_1 = t$. For this low order correlation, the time ordering (17) sets no additional conditions. There are two possibilities for τ_1, depending on whether time t or t' is later. Consider first $t' \geqslant t$, so that $\tau_1 = t$, $\tau_2 = t'$. Using (20) and (19) we have that

$$\langle \widehat{a}_j^\dagger(t')\widehat{a}_k(t)\rangle = \mathrm{Tr}\left[\breve{V}(t',t)\left\{\widehat{a}_k(t)\widehat{\rho}(t)\right\}\widehat{a}_j^\dagger(t')\right] \tag{23}$$

$$= \mathrm{Tr}\left[\widehat{a}_j^\dagger(t')\breve{V}(t',t)\left\{\widehat{a}_k(t)\widehat{\rho}(t)\right\}\right] \tag{24}$$

The 2nd line follows from the cyclic property of traces. The $\{\cdot\}$ is kept for now for clarity. We can see that the evolution operator from t to t' acts to the right on all the quantities at time t, while the later-time operator $\widehat{a}_j^\dagger(t')$ acts only on the evolved quantities to its right. This makes intuitive physical sense. In the second case of $t' < t$, we have $\tau_1 = t'$, $\tau_2 = t$, and get that

$$\langle \widehat{a}_j^\dagger(t')\widehat{a}_k(t)\rangle = \mathrm{Tr}\left[\widehat{a}_k(t)\breve{V}(t,t')\left\{\widehat{\rho}(t')\widehat{a}_j^\dagger(t')\right\}\right]. \tag{25}$$

This again has the intuitive form of the operator $\breve{V}$ acting to the right on all the earlier-time quantities.

Take the first case with $t' \geqslant t$. Expressing the density matrix in (24) in the positive-P representation (2a),

$$G^{(1)} = \mathrm{Tr}\left[\widehat{a}_j^\dagger(t')\breve{V}(t',t)\left\{\int d^{4M}\boldsymbol{\lambda}\, P_+(\boldsymbol{\lambda},t)\,\widehat{a}_k(t)\widehat{\Lambda}(\boldsymbol{\lambda})\right\}\right]$$

$$= \mathrm{Tr}\left[\widehat{a}_j^\dagger(t')\breve{V}(t',t)\left\{\int d^{4M}\boldsymbol{\lambda}\,\alpha_k P_+(\boldsymbol{\lambda},t)\,\widehat{\Lambda}(\boldsymbol{\lambda})\right\}\right]. \tag{26}$$

The 2nd line follows from application of (5a). We cannot do the same for $\widehat{a}_j^\dagger(t')$ yet, because the kernel $\widehat{\Lambda}$ finds itself inside the prior action of the $\breve{V}$ operator.

To deal with this, consider now the action of the evolution operator $\breve{V}$ on distributions P_+. i.e. the action of the PDE (7). If we define the conditional distribution $\mathcal{P}(\boldsymbol{\lambda},t'|\underline{\boldsymbol{\lambda}},t)$ as the solution of this PDE at time $t' \geqslant t$ starting from the initial condition $\delta^{4M}(\boldsymbol{\lambda}-\underline{\boldsymbol{\lambda}})$, i.e. the "propagator", then it can be used to formally write

$$\breve{V}(t',t)\left\{\int d^{4M}\boldsymbol{\lambda}\, P_+(\boldsymbol{\lambda},t)\widehat{\Lambda}(\boldsymbol{\lambda})\right\}$$

$$= \breve{V}(t',t)\left\{\int d^{4M}\boldsymbol{\lambda}\int d^{4M}\underline{\boldsymbol{\lambda}}\,\delta^{4M}(\boldsymbol{\lambda}-\underline{\boldsymbol{\lambda}})\,P_+(\underline{\boldsymbol{\lambda}},t)\widehat{\Lambda}(\boldsymbol{\lambda})\right\}$$

$$= \int d^{4M}\boldsymbol{\lambda}\int d^{4M}\underline{\boldsymbol{\lambda}}\,\mathcal{P}(\boldsymbol{\lambda},t'|\underline{\boldsymbol{\lambda}},t)P_+(\underline{\boldsymbol{\lambda}},t)\widehat{\Lambda}(\boldsymbol{\lambda}). \tag{27}$$

This now contains no more two-sided operators. Through this convolution, P_+ is expressed in $\underline{\boldsymbol{\lambda}}$ variables which accompany the earliest time t to aid for later interpretation as part of a joint probability, while the kernel $\widehat{\Lambda}$ is expressed in the variables $\boldsymbol{\lambda}$ that accompany later times, ready for application of the next operator identity.

Notice that there are no particularly stringent assumptions about P_+ for (27) itself to apply. For example, (27) applies equally well if one replaces P_+ with some complex distribution function $\widetilde{P}$. This point will soon be useful. However, there *was* an assumption that the propagator $\mathcal{P}$ is well behaved. This is certainly true if the PDE was of a Fokker-Planck form (8), and therefore is always justified if we have an exact mapping of the master equation (6) to stochastic equations (9). However, in some other cases of third/higher order terms in the PDE, it might not. We will not be concerned with such cases here.

Now in (26), $\breve{V}$ is acting on a distribution $\widetilde{P}(\boldsymbol{\lambda},t) = \alpha_k P_+(\boldsymbol{\lambda},t)$. Using (27) we get

$$G^{(1)} = \mathrm{Tr}\left[\widehat{a}_j^\dagger(t')\int d^{4M}\boldsymbol{\lambda}\int d^{4M}\underline{\boldsymbol{\lambda}}\mathcal{P}(\boldsymbol{\lambda},t'|\underline{\boldsymbol{\lambda}},t)\widetilde{P}(\underline{\boldsymbol{\lambda}},t)\,\widehat{\Lambda}(\boldsymbol{\lambda})\right]$$

$$= \mathrm{Tr}\left[\widehat{a}_j^\dagger(t')\int d^{4M}\boldsymbol{\lambda}\int d^{4M}\underline{\boldsymbol{\lambda}}\,\underline{\alpha}_k\mathcal{P}(\boldsymbol{\lambda},t'|\underline{\boldsymbol{\lambda}},t)P_+(\underline{\boldsymbol{\lambda}},t)\,\widehat{\Lambda}(\boldsymbol{\lambda})\right]. \tag{28}$$

The two-way operator acting on the right that was $\breve{V}$, has now been gotten rid of, by virtue of being incorporated in the propagator $\mathcal{P}$. Therefore, the remaining operator $\widehat{a}_j^\dagger$ can now be shifted to the right due to the cyclic property of the trace, and then processed via (5d) as so:

$$G^{(1)} = \int d^{4M}\boldsymbol{\lambda}\int d^{4M}\underline{\boldsymbol{\lambda}}\mathcal{P}(\boldsymbol{\lambda},t'|\underline{\boldsymbol{\lambda}},t)\widetilde{P}(\underline{\boldsymbol{\lambda}},t)\,\mathrm{Tr}\left[\widehat{\Lambda}(\boldsymbol{\lambda})\widehat{a}_j^\dagger(t')\right]$$

$$= \int d^{4M}\boldsymbol{\lambda}\,\beta_j\int d^{4M}\underline{\boldsymbol{\lambda}}\,\underline{\alpha}_k\mathcal{P}(\boldsymbol{\lambda},t'|\underline{\boldsymbol{\lambda}},t)P_+(\underline{\boldsymbol{\lambda}},t)\,\mathrm{Tr}\left[\widehat{\Lambda}(\boldsymbol{\lambda})\right]$$

$$= \int d^{4M}\boldsymbol{\lambda}\,\beta_j\int d^{4M}\underline{\boldsymbol{\lambda}}\,\underline{\alpha}_k\mathcal{P}(\boldsymbol{\lambda},t'|\underline{\boldsymbol{\lambda}},t)P_+(\underline{\boldsymbol{\lambda}},t). \tag{29a}$$

The last line follows from $\mathrm{Tr}\left[\widehat{\Lambda}\right] = 1$, which is pre-set by the definition (2b).

The quantity $\mathcal{P}P_+$ is the just the joint probability

$$P(\boldsymbol{\lambda},t';\underline{\boldsymbol{\lambda}},t) = \mathcal{P}(\boldsymbol{\lambda},t'|\underline{\boldsymbol{\lambda}},t)P_+(\underline{\boldsymbol{\lambda}},t) \tag{30}$$

of having configuration $\underline{\boldsymbol{\lambda}}$ at time t and configuration $\boldsymbol{\lambda}$ at time t'. (Provided $\mathcal{P}$ is well behaved, positive, real, as mentioned before, which is the case for any model fully described by an FPE (8)). Therefore,

$$G^{(1)} = \int d^{4M}\boldsymbol{\lambda}\int d^{4M}\underline{\boldsymbol{\lambda}}\;\beta_j\underline{\alpha}_k\;P(\boldsymbol{\lambda},t';\underline{\boldsymbol{\lambda}},t). \tag{31}$$

At this stage we can identify probability with stochastic realisations. The noises $\xi_\mu(t)$ introduced during time evolution are independent from each other, independent at each time step, independent for each sample's trajectory. They are also independent of any other

random variables used to produce the initial ensemble $\{\boldsymbol{\lambda}^{(1)},\ldots,\boldsymbol{\lambda}^{(\mathcal{S})}\}(t)$ that samples $P_+(\boldsymbol{\lambda},t)$. Therefore, the evolved configuration $\boldsymbol{\lambda}^{(u)}(t')$ at time t' depends only on mutually independent random variables that consist of $\boldsymbol{\lambda}^{(u)}(t)$ and the noise history of the uth trajectory. As a result, the combination of initial configuration $\boldsymbol{\lambda}^{(u)}(t)$ and the evolved configuration $\boldsymbol{\lambda}^{(u)}(t')$, together form an unbiased sample of the joint distribution $P(\boldsymbol{\lambda},t';\underline{\boldsymbol{\lambda}},t)$. We arrive then at the final result that

$$G^{(1)}(t',t)=\langle\widehat{a}_j^\dagger(t')\widehat{a}_k(t)\rangle=\langle\beta_j(t')\alpha_k(t)\rangle_{\rm stoch}. \quad (32)$$

The procedure for the case $t'<t$ gives a result analogous to (31):

$$G^{(1)}=\int d^{4M}\boldsymbol{\lambda}\int d^{4M}\underline{\boldsymbol{\lambda}}\;\underline{\beta}_j\alpha_k\;P(\boldsymbol{\lambda},t;\underline{\boldsymbol{\lambda}},t'), \quad (33)$$

which once again leads to (32).

It is especially important to note that the quantity to be averaged comes from the *time evolution of individual sample trajectories*. Explicitly:

$$\langle\widehat{a}_j^\dagger(t')\widehat{a}_k(t)\rangle=\lim_{\mathcal{S}\to\infty}\frac{1}{\mathcal{S}}\sum_{u=1}^{\mathcal{S}}\beta_j^{(u)}(t')\alpha_k^{(u)}(t). \quad (34)$$

This allows for very efficient calculations.

3.1.2 Higher order correlations

Other time and normal ordered correlations follow a similar pattern. For example, when $t''\geqslant t'\geqslant t$,

$$\langle\widehat{a}_j(t'')\widehat{a}_k(t')\widehat{a}_l(t)\rangle \quad (35)$$
$$=\mathrm{Tr}\left[\widehat{a}_j(t'')\breve{V}(t'',t')\left\{\widehat{a}_k(t')\breve{V}(t',t)\left\{\widehat{a}_l(t)\widehat{\rho}(t)\right\}\right\}\right].$$

In this case, following a similar procedure to before, one can act alternately with (5a) on the kernel to extract a factor of α, and (27) to convert the evolution operators to propagators. One finds

$$\langle\widehat{a}_j(t'')\widehat{a}_k(t')\widehat{a}_l(t)\rangle=\int d^{4M}\boldsymbol{\lambda}d^{4M}\underline{\boldsymbol{\lambda}}d^{4M}\underline{\underline{\boldsymbol{\lambda}}}\;\alpha_j\underline{\alpha}_k\underline{\underline{\alpha}}_l$$
$$\times\mathcal{P}(\boldsymbol{\lambda},t''|\underline{\boldsymbol{\lambda}},t')\mathcal{P}(\underline{\boldsymbol{\lambda}},t'|\underline{\underline{\boldsymbol{\lambda}}},t)P_+(\underline{\underline{\boldsymbol{\lambda}}},t). \quad (36)$$

Since the times are ordered $t''\geqslant t'\geqslant t$, and the conditional probabilities follow from the evolution of the FPE, $\underline{\underline{\boldsymbol{\lambda}}}$ are parent variables of the $\underline{\boldsymbol{\lambda}}$ and so on, and the product of conditional probabilities is just the joint probability. Hence (36) is

$$\int d^{4M}\boldsymbol{\lambda}d^{4M}\underline{\boldsymbol{\lambda}}d^{4M}\underline{\underline{\boldsymbol{\lambda}}}\;\alpha_j\underline{\alpha}_k\underline{\underline{\alpha}}_l\;P(\boldsymbol{\lambda},t'';\underline{\boldsymbol{\lambda}},t';\underline{\underline{\boldsymbol{\lambda}}},t), \quad (37)$$

and

$$\langle\widehat{a}_j(t'')\widehat{a}_k(t')\widehat{a}_l(t)\rangle=\langle\alpha_j(t'')\alpha_k(t')\alpha_l(t)\rangle_{\rm stoch}. \quad (38)$$

Working similarly, using just the 1st and 4th identities in (5), one readily but somewhat cumbersomely finds that the stochastic estimator for the general time-and-normal-ordered correlation function is

$$\langle\widehat{a}_{p_1}^\dagger(t_1)\cdots\widehat{a}_{p_\mathcal{N}}^\dagger(t_\mathcal{N})\widehat{a}_{q_1}(s_1)\cdots\widehat{a}_{q_\mathcal{M}}(s_\mathcal{M})\rangle$$
$$=\langle\beta_{p_1}(t_1)\cdots\beta_{p_\mathcal{N}}(t_\mathcal{N})\alpha_{q_1}(s_1)\cdots\alpha_{q_\mathcal{M}}(s_\mathcal{M})\rangle_{\rm stoch}. \quad (39)$$

Here, of course (17) must hold, and the stochastic averaging is over products constructed using values from the evolution of a single sample, as in (34). It confirms the suspicion and intuition that the behaviour of the positive-P representation in this regard should be similar to the earlier expression (21), for the Glauber-Sudarshan P.

3.2 Other ordering in the positive-P

Now to see the limitations of this scheme, consider the anti-normally (but time-ordered) ordered correlation

$$\mathcal{A}=\langle\widehat{a}_j(t')\widehat{a}_k^\dagger(t)\rangle \quad (40)$$

with $t'>t$. The first point to make is that we cannot rearrange this to a normal-ordered form like $\langle\widehat{a}_k^\dagger(t)\widehat{a}_j(t')+\delta_{jk}\rangle$ and then use (39) because generally $\left[\widehat{a}_j(t'),\widehat{a}_k^\dagger(t)\right]\neq\delta_{jk}$ when $t\neq t'$. Instead it is some time-dependent operator. Now applying (20), (40) can be written

$$\mathcal{A}=\langle\widehat{a}_j(t')\widehat{a}_k^\dagger(t)\rangle=\mathrm{Tr}\left[\widehat{a}_j(t')\breve{V}(t',t)\left\{\widehat{a}_k^\dagger(t)\widehat{\rho}(t)\right\}\right]. \quad (41)$$

Upon expansion, we will need to act on $\widehat{\Lambda}$ using the 2nd identity in (5), (5b), to convert $\widehat{a}_k^\dagger$ to variable form. Thus

$$\mathcal{A}=\mathrm{Tr}\left[\widehat{a}_j(t')\breve{V}(t',t)\Big\{\right.$$
$$\left.\int d^{4M}\boldsymbol{\lambda}\,P_+(\boldsymbol{\lambda},t)\;\left[\beta_k+\frac{\partial}{\partial\alpha_k}\right]\widehat{\Lambda}(\boldsymbol{\lambda})\Big\}\right]. \quad (42)$$

This is not of a form amenable to (27). We can soldier on applying integration by parts and assuming negligible boundary terms to obtain

$$\mathcal{A}=\mathrm{Tr}\left[\widehat{a}_j(t')\breve{V}(t',t)\Big\{\right. \quad (43)$$
$$\left.\int d^{4M}\boldsymbol{\lambda}\;\left[\beta_kP_+(\boldsymbol{\lambda},t)-\frac{\partial P_+(\boldsymbol{\lambda},t)}{\partial\alpha_k}\right]\widehat{\Lambda}(\boldsymbol{\lambda})\Big\}\right].$$

The matter of whether boundary terms can be discarded has been studied in depth [23, 34, 37, 66, 85, 126]. The summary is that one can determine operationally in a

stochastic simulation whether boundary terms are negligible or not. If deemed negligible, then integration by parts is justified. In (43) we can now identify a distribution $\widetilde{P}(\boldsymbol{\lambda},t)=[\beta_k-\frac{\partial}{\partial\alpha_k}]P_+(\boldsymbol{\lambda},t)$ to act on with (27). Doing so gives:

$$\mathcal{A}=\mathrm{Tr}\Bigg[\widehat{a}_j(t')\int\int d^{4M}\boldsymbol{\lambda}\,d^{4M}\underline{\boldsymbol{\lambda}} \tag{44}$$
$$\mathcal{P}(\boldsymbol{\lambda},t'|\underline{\boldsymbol{\lambda}},t)\left[\underline{\beta}_k P_+(\underline{\boldsymbol{\lambda}},t)-\frac{\partial P_+(\underline{\boldsymbol{\lambda}},t)}{\partial\underline{\alpha}_k}\right]\widehat{\Lambda}(\boldsymbol{\lambda})\Bigg].$$

The second operator $\widehat{a}_j(t')$ can now act on $\widehat{\Lambda}$ from the left. One obtains

$$\mathcal{A}=\int\int d^{4M}\boldsymbol{\lambda}\,d^{4M}\underline{\boldsymbol{\lambda}} \tag{45}$$
$$\mathcal{P}(\boldsymbol{\lambda},t'|\underline{\boldsymbol{\lambda}},t)\alpha_j\left[\underline{\beta}_k P_+(\underline{\boldsymbol{\lambda}},t)-\frac{\partial P_+(\underline{\boldsymbol{\lambda}},t)}{\partial\underline{\alpha}_k}\right].$$

While this is formally acceptable (given those negligible boundary terms), and could be used for some analytic work in small systems such as demonstrated in [62], unfortunately the derivative of P_+ is not amenable to interpretation in terms of stochastic samples. At least not the direct samples we are investigating here. It may be partially treatable using the quantum jump and response theory approach previously applied to truncated Wigner [13, 115, 118], which is a topic for another time.

However – in Sections 5 and 6, a different direct way to evaluate anti-normal ordered observables such as $\mathcal{A}=\langle\widehat{a}_j(t')\widehat{a}_k^\dagger(t)\rangle$ will be demonstrated.

4 Other phase-space representations

In the derivations of Sec. 3.1, one can see that the crucial aspect for obtaining a stochastically useful expression is to use only those identities which do not contain derivatives[1]. This suggests that convenient expressions for multi-time correlations similar to (39) will be obtainable whenever the operators in the correlation can be converted to phase-space variables without resorting to identities with derivatives.

However, it happens that such identities without derivatives are not particularly abundant in other phase-space representations. For example, the Wigner representation [105, 118, 141] has derivatives in all identities, as does its dimension-doubled analogue [71, 116].

[1]Strictly speaking, a small exception to this appears if the derivative appears only at the final time when the only remaining operator is $\widehat{\Lambda}$ since $\mathrm{Tr}[\frac{\partial}{\partial\lambda_\mu}\widehat{\Lambda}]=\frac{\partial}{\partial\lambda_\mu}\mathrm{Tr}[\widehat{\Lambda}]=0$ removes any awkward terms. Such a case can, however, also be treated by an identity without any derivatives after using the cyclic property of the trace at the right step.

Notably, while the trace of the symmetric form in the Wigner representation corresponds to $|\alpha|^2$ with no corrections: $\mathrm{Tr}\left[\frac{1}{2}\left(\widehat{a}^\dagger\widehat{a}+\widehat{a}\widehat{a}^\dagger\right)\widehat{\Lambda}_{\mathrm{Wig}}\right]=|\alpha|^2$, this does not remove derivatives in the corresponding identity[2]. The best that appears to be achievable in this way is

$$\frac{\widehat{a}^\dagger\widehat{a}+\widehat{a}\widehat{a}^\dagger}{2}\widehat{\Lambda}_{\mathrm{Wig}}=\left[|\alpha|^2+\frac{1}{4}\frac{\partial^2}{\partial\alpha\partial\alpha^*}\right]\widehat{\Lambda}_{\mathrm{Wig}}. \tag{46}$$

Hence, the path-integral and time-symmetric approach [13] is more suited to the Wigner representation. Also the phase-space representations developed for spin systems [11, 100, 107], contain derivatives for all identities.

One notable exception is the Q representation, which admits derivative-free identities similar to (5) for *anti*-normally ordered operators, and so is a good candidate for convenient phase-space expressions. Time-ordered anti-normal operators occur for example in the theory of photon detectors that operate via emission rather than absorption of photons [99]. Formal integral expressions for this kind of correlation were also provided in [5]. Below, the operational stochastic expressions are found using the Gardiner approach.

4.1 The case of the Q representation

The Husimi Q representation [75] is defined as

$$Q(\boldsymbol{\alpha})=\frac{1}{\pi^M}\langle\boldsymbol{\alpha}|\,\widehat{\rho}\,|\boldsymbol{\alpha}\rangle \tag{47}$$

and is positive for any $\widehat{\rho}$. Due to the Q distribution being defined in this explicit way, rather than the implicit form (2), observable expressions in the Q distribution have traditionally been found by simply expanding the trace:

$$\mathrm{Tr}\left[\widehat{O}\,\widehat{\rho}\right]=\frac{1}{\pi^M}\int d^{2M}\boldsymbol{\alpha}\;\langle\boldsymbol{\alpha}|\widehat{O}\,\widehat{\rho}\,|\boldsymbol{\alpha}\rangle, \tag{48}$$

and applying the eigenvalue equation for coherent states

$$\widehat{a}_j|\boldsymbol{\alpha}\rangle=\alpha_j|\boldsymbol{\alpha}\rangle. \tag{49}$$

For anti-normal ordered correlations at equal times, the cyclic property of traces gives $\langle\widehat{a}_{j_1}\cdots\widehat{a}_{j_\mathcal{N}}\widehat{a}^\dagger_{k_1}\cdots\widehat{a}^\dagger_{k_\mathcal{M}}\rangle=\mathrm{Tr}\left[\widehat{a}^\dagger_{k_1}\cdots\widehat{a}^\dagger_{k_\mathcal{M}}\widehat{\rho}\,\widehat{a}_{j_1}\cdots\widehat{a}_{j_\mathcal{N}}\right]$ which immediately leads to

$$\langle\widehat{a}_{j_1}\cdots\widehat{a}_{j_\mathcal{N}}\widehat{a}^\dagger_{k_1}\cdots\widehat{a}^\dagger_{k_\mathcal{M}}\rangle=\langle\alpha_{j_1}\cdots\alpha_{j_\mathcal{N}}\alpha^*_{k_1}\cdots\alpha^*_{k_\mathcal{M}}\rangle_{\mathrm{stoch}}. \tag{50}$$

However, this traditional approach fails with time-ordered correlations. Whatever way one orders the operators, working this way on expression (20) will lead

[2]Here, $\widehat{\Lambda}_{\mathrm{Wig}}=\widehat{\Lambda}_s$ from (53) with $s=0$.

to a form

$$\frac{1}{\pi^M}\int d^{2M}\boldsymbol{\alpha}\langle\boldsymbol{\alpha}|\Big[\breve{F}_R \tag{51}$$

$$\breve{V}(\tau_R,\tau_{R-1})\Big\{\breve{F}_{R-1}\breve{V}(\tau_{R-1},\tau_{R-2})\big\{\cdots\breve{F}_1\widehat{\rho}(\tau_1)\big\}\Big\}\Big]|\boldsymbol{\alpha}\rangle$$

in which it is the *latest time* operator $\breve{F}_R(\tau_R)$ that acts on the outer coherent states. One can convert $\breve{F}_R$ to phase-space variables using (49), and move the state vectors $|\boldsymbol{\alpha}\rangle$ or $\langle\boldsymbol{\alpha}|$ closer to the density matrix and the form (47). However, in the next putative step, there is no clear way to convert the evolution operator $\breve{V}(\tau_R,\tau_{R-1})$ to phase space form. Moreover, when there is phase-space diffusion, the propagator $\mathcal{P}$ is well-behaved only in the forward time direction, so there is no way to act with $\mathcal{P}$ on the outer state vectors and variables which correspond to later times than the inner ones.

Therefore, we proceed in a non-traditional way, using an implicit form similar to what was done for the positive-P distribution in Sec. 3.1. The Q representation is the $s\to-1$ limiting case of the family of s-ordered representations $W_s(\boldsymbol{\alpha})$ studied by Cahill and Glauber [19, 20] (the Glauber-Sudarshan P and Wigner correspond to $s=1$ and $s=0$, respectively). All these distributions can be written using coherent displacement operators

$$\widehat{D}_j(\alpha_j)=e^{\alpha_j\widehat{a}_j^\dagger-\alpha_j^*\widehat{a}_j},\ ;\ \widehat{D}(\boldsymbol{\alpha})=\prod_j\widehat{D}_j(\alpha_j), \tag{52}$$

in an implicit form similar to (2):

$$\widehat{\rho}=\int d^{2M}\boldsymbol{\alpha}\,W_s(\boldsymbol{\alpha})\widehat{\Lambda}_s(\boldsymbol{\alpha}) \tag{53a}$$

$$\widehat{\Lambda}_s(\boldsymbol{\alpha})=\prod_j\widehat{D}_j(\alpha_j)\widehat{T}_j(0,-s)\widehat{D}_j(-\alpha_j), \tag{53b}$$

with the base operator [20]

$$\widehat{T}_j(0,-s)=\frac{2}{1+s}\left(\frac{s-1}{1+s}\right)^{\widehat{a}_j^\dagger\widehat{a}_j}. \tag{54}$$

One has $\mathrm{Tr}\left[\widehat{\Lambda}_s\right]=1$ and the operator identities

$$\widehat{a}_j\widehat{\Lambda}_s=\left[\alpha_j-\frac{1-s}{2}\frac{\partial}{\partial\alpha_j^*}\right]\widehat{\Lambda}_s, \tag{55a}$$

$$\widehat{a}_j^\dagger\widehat{\Lambda}_s=\left[\alpha_j^*+\frac{1+s}{2}\frac{\partial}{\partial\alpha_j}\right]\widehat{\Lambda}_s, \tag{55b}$$

$$\widehat{\Lambda}_s\widehat{a}_j=\left[\alpha_j+\frac{1+s}{2}\frac{\partial}{\partial\alpha_j^*}\right]\widehat{\Lambda}_s, \tag{55c}$$

$$\widehat{\Lambda}_s\widehat{a}_j^\dagger=\left[\alpha_j^*-\frac{1-s}{2}\frac{\partial}{\partial\alpha_j}\right]\widehat{\Lambda}_s, \tag{55d}$$

which can be verified by equating the LHS and RHS when $\widehat{T}(0,-s)$ is expanded in number states. Therefore, in the limit $s\to-1$ corresponding to the Q representation with $\widehat{\Lambda}_{-1}=\widehat{\Lambda}_Q$,

$$\widehat{a}_j\widehat{\Lambda}_Q=\left[\alpha_j-\frac{\partial}{\partial\alpha_j^*}\right]\widehat{\Lambda}_Q, \tag{56a}$$

$$\widehat{a}_j^\dagger\widehat{\Lambda}_Q=\alpha_j^*\widehat{\Lambda}_Q, \tag{56b}$$

$$\widehat{\Lambda}_Q\widehat{a}_j=\alpha_j\widehat{\Lambda}_Q, \tag{56c}$$

$$\widehat{\Lambda}_Q\widehat{a}_j^\dagger=\left[\alpha_j^*-\frac{\partial}{\partial\alpha_j}\right]\widehat{\Lambda}_Q. \tag{56d}$$

We see then that multi-time correlations in which only the orderings $\widehat{a}_j^\dagger\widehat{\Lambda}_Q$ and $\widehat{\Lambda}_Q\widehat{a}_j$ appear could have the capacity to correspond to simple stochastic expressions. This implies anti-normal ordered moments since by the cyclic property of traces

$$\mathrm{Tr}\left[\widehat{a}_{q_1}^\dagger\cdots\widehat{a}_{q_\mathcal{M}}^\dagger\widehat{\rho}\,\widehat{a}_{p_1}\cdots\widehat{a}_{p_\mathcal{N}}\right]=\langle\widehat{a}_{p_1}\cdots\widehat{a}_{p_\mathcal{N}}\widehat{a}_{q_1}^\dagger\cdots\widehat{a}_{q_\mathcal{M}}^\dagger\rangle. \tag{57}$$

The implicit form (53) for $\widehat{\rho}$ allows us to proceed in a similar fashion to Sec. 3.1. Consider then the anti-normal and time-ordered correlation

$$\mathcal{A}'=\langle\widehat{a}_{p_1}(t_1)\cdots\widehat{a}_{p_\mathcal{N}}(t_\mathcal{N})\widehat{a}_{q_1}^\dagger(s_1)\cdots\widehat{a}_{q_\mathcal{M}}^\dagger(s_\mathcal{M})\rangle \tag{58}$$

with times obeying (17). A potentially awkward issue is that the kernel $\widehat{\Lambda}_s$ is not very well bounded in the $s\to-1$ limit, with $\langle\boldsymbol{\beta}|\widehat{\Lambda}_s(\boldsymbol{\alpha})|\boldsymbol{\beta}\rangle=\frac{2}{\varepsilon}\exp\left[-2|\boldsymbol{\alpha}-\boldsymbol{\beta}|^2/\varepsilon\right]$ where $s=\varepsilon-1$. To gauge whether this is a problem, we will work using infinitesimal $\varepsilon>0$ in which case

$$\widehat{\Lambda}_s\to\widehat{\Lambda}_Q+\mathcal{O}(\varepsilon). \tag{59}$$

Using the form (20) on (57) with now $B=\widehat{a}^\dagger$ and $A=\widehat{a}$, one obtains

$$\mathcal{A}'=\mathcal{O}(\varepsilon)+\int d^{2M}\boldsymbol{\alpha}\,\mathrm{Tr}\Big[\breve{F}_R\breve{V}(\tau_R,\tau_{R-1})\Big\{ \tag{60}$$

$$\cdots\breve{F}_3\breve{V}(\tau_3,\tau_2)\Big\{\breve{F}_2\breve{V}(\tau_2,\tau_1)\big\{W_s(\boldsymbol{\alpha},\tau_1)\breve{F}_1\widehat{\Lambda}_Q(\boldsymbol{\alpha})\big\}\Big\}\Big\}\Big].$$

The part in the inner { } brackets will be either

$$\begin{array}{ll}W_s(\boldsymbol{\alpha},t_1)\widehat{\Lambda}_Q\widehat{a}_{p_1} & \text{if } t_1\leqslant s_\mathcal{M}\\ W_s(\boldsymbol{\alpha},s_\mathcal{M})\widehat{a}_{q_\mathcal{M}}^\dagger\widehat{\Lambda}_Q & \text{otherwise.}\end{array} \tag{61}$$

Both cases allow us to use derivative-free identities (56c) or (56b), to replace (61) with $\widetilde{P}_s(\boldsymbol{\alpha},\tau_1)\widehat{\Lambda}_Q$ where

$$\begin{array}{ll}\widetilde{P}_s=\alpha_{p_1}W_s(\boldsymbol{\alpha},s_\mathcal{M}) & \text{if } t_1\leqslant s_\mathcal{M}\\ \widetilde{P}_s=\alpha_{q_\mathcal{M}}^*W_s(\boldsymbol{\alpha},t_1) & \text{otherwise.}\end{array} \tag{62}$$

Now assuming an acceptable propagator $\mathcal{P}_s(\boldsymbol{\alpha},\tau_2|\underline{\boldsymbol{\alpha}},\tau_1)$ exists for the evolution of the s-ordered distribution W_s, use of (27) leads to

$$\mathcal{A}' = \mathcal{O}(\varepsilon) + \int d^{2M}\boldsymbol{\alpha} \int d^{2M}\underline{\boldsymbol{\alpha}}\,\mathrm{Tr}\Big[\breve{F}_R\breve{V}(\tau_R,\tau_{R-1})\Big\{ \cdots \breve{F}_3\breve{V}(\tau_3,\tau_2)\Big\{\mathcal{P}_s(\boldsymbol{\alpha},\tau_2|\underline{\boldsymbol{\alpha}},\tau_1)\widetilde{P}_s(\underline{\boldsymbol{\alpha}},\tau_1)\breve{F}_2\widehat{\Lambda}_Q\Big\}\Big\}\Big], \quad (63)$$

in which the objects related to the first time interval have been fully converted to phase-space quantities. Proceeding in this fashion with increasing time for the remaining $\widehat{a}$ and $\widehat{a}^\dagger$ operators, one arrives at

$$\mathcal{A}' = \Big[\int d^{2M}\boldsymbol{\alpha}(\tau_1)\int d^{2M}\boldsymbol{\alpha}(\tau_2)\cdots\int d^{2M}\boldsymbol{\alpha}(\tau_R) \alpha_{p_1}(t_1)\cdots\alpha_{p_\mathcal{N}}(t_\mathcal{N})\alpha^*_{q_1}(s_1)\cdots\alpha^*_{q_\mathcal{M}}(s_\mathcal{M})\times \mathcal{P}_s(\boldsymbol{\alpha}(\tau_R),\tau_R|\boldsymbol{\alpha}(\tau_{R-1}),\tau_{R-1})\cdots\mathcal{P}_s(\boldsymbol{\alpha}(\tau_2),\tau_2|\boldsymbol{\alpha}(\tau_1),\tau_1) \times W_s(\boldsymbol{\alpha}(\tau_1),\tau_1)\Big] + \mathcal{O}(\varepsilon). \quad (64)$$

Variables $\boldsymbol{\alpha},\underline{\boldsymbol{\alpha}}$ etc were relabelled to $\boldsymbol{\alpha}(\tau_R),\boldsymbol{\alpha}(\tau_{R-1})$.

In the limit $\varepsilon\to 0$ that we are considering, $W_s(\boldsymbol{\alpha})\to Q(\boldsymbol{\alpha})$, which is real non-negative. To be consistent, the propagator $\mathcal{P}_{-1}$ must also be real nonnegative. When the master equation (6) is faithfully reproduced by a Fokker-Planck equation for $Q(\boldsymbol{\alpha})$, this will be the case. Then, the $\mathcal{P}_s\ldots\mathcal{P}_sW_s$ factors can be interpreted similarly to (30) as the joint probability of samples $\boldsymbol{\alpha}(\tau_1),\boldsymbol{\alpha}(\tau_2),\ldots$ at successive times. With that, we arrive at the hoped for result that a time ordered (as (17)) and *anti*-normally ordered correlation is evaluated as

$$\langle\widehat{a}_{p_1}(t_1)\cdots\widehat{a}_{p_\mathcal{N}}(t_\mathcal{N})\widehat{a}^\dagger_{q_1}(s_1)\cdots\widehat{a}^\dagger_{q_\mathcal{M}}(s_\mathcal{M})\rangle = \langle\alpha_{p_1}(t_1)\cdots\alpha_{p_\mathcal{N}}(t_\mathcal{N})\alpha^*_{q_1}(s_1)\cdots\alpha^*_{q_\mathcal{M}}(s_\mathcal{M})\rangle_{\mathrm{stoch}} \quad (65)$$

using Q *representation* samples α_j. Stochastic averaging is over products constructed using values from the evolution of a single sample, like in (34).

5 Evaluation by conversion to the Q representation

5.1 Conversion between samples of s-ordered distributions

The s-ordered distributions W_s introduced in (53) are mutually related by [20]

$$W_s(\boldsymbol{\alpha}') = \left(\frac{2}{s_0-s}\right)^M\int\frac{d^{2M}\boldsymbol{\alpha}}{\pi^M}\exp\left[-\frac{2|\boldsymbol{\alpha}'-\boldsymbol{\alpha}|^2}{s_0-s}\right]W_{s_0}(\boldsymbol{\alpha}). \quad (66)$$

in the sense that W_s and W_{s_0} represent the same quantum density matrix $\widehat{\rho}$. When $s_0>s$, this is a Gaussian convolution of the more normally-ordered distribution W_{s_0}, and reflects the well known property that Q distributions ($s=-1$) are broader and more smoothed than Wigner ($s=0$), which are in turn broader than Glauber-Sudarshan P distributions ($s=1$) for the same state. Importantly for us here, this means that if we have samples $\boldsymbol{\alpha}$ of a more normally ordered distribution, we can easily also obtain samples $\boldsymbol{\alpha}'$ of the less normally ordered distributions simply by adding Gaussian noise. The prescription is

$$\alpha'_j = \alpha_j + \sqrt{\frac{s_0-s}{2}}\,\zeta_j \quad (67)$$

for each mode j, with each ζ_j a complex random variable of variance 1:

$$\langle\zeta_j\rangle_{\mathrm{stoch}} = 0\ ;\ \langle\zeta_j\zeta_k\rangle_{\mathrm{stoch}} = 0\ ;\ \langle\zeta^*_j\zeta_k\rangle_{\mathrm{stoch}} = 1. \quad (68)$$

In particular, converting samples of a P distribution to samples of Q requires

$$\alpha'_j = \alpha_j + \zeta_j. \quad (69)$$

Converting samples of a Wigner distribution (if it is nonnegative to begin with) to samples of Q can be done with

$$\alpha'_j = \alpha^{\mathrm{Wig}}_j + \frac{\zeta_j}{\sqrt{2}}. \quad (70)$$

5.2 Evaluation of anti-normal ordered moments starting from P and Wigner representations

Therefore, if one has samples $\boldsymbol{\alpha}(t_0)$ of a P or Wigner representation up to a time t_0 (e.g. from a prior stochastic evolution), the prescription (67) can be used to convert them to samples $\boldsymbol{\alpha}'(t_0)$ of the Q representation at that time. The noises ζ_j are generated just once at this time. Subsequent evolution according to the Q stochastic equations then leads to Q samples $\boldsymbol{\alpha}'(t)$ at later times $t>t_0$. These can be directly used in expression (65) to evaluate anti-normal ordered multi-time observables.

This is potentially a little less convenient that remaining in one distribution throughout because the conversion time t_0 has to be chosen before starting a simulation, and the anti-normal ordered operators cannot extend to times before t_0. It does preserve the principal advantages of phase-space simulation, though: intuitive and computationally tractable expressions for observables, stochasticity, gentle scaling with system size. The evolution equations (9) are usually of similar form in all s-ordered representations, apart from simplification at special s values.

One cannot convert the other way with this procedure (e.g. from Wigner to P), so normally ordered multi-time correlations cannot be extracted this way from samples of Wigner or Q distributions.

5.3 Mixed-order moments

The above discussion suggests a way that some mixed-order multi-time correlations that contain both normal and anti-normal factors could be evaluated. Suppose early time operators ($t \leqslant t_0$) are normally ordered (can be evaluated using the P distribution), while later time operators ($t > t_0$) are anti-normally ordered (can be evaluated using the Q representation). A switch according to (69) could be made at t_0 after evaluating any normally-ordered factors, and the Q distribution evolved and used at later times to obtain the remaining inner factors with $t > t_0$. Let us check in detail whether this is feasible.

Consider the time-ordered but neither anti- or normally ordered correlation

$$\begin{aligned}\mathcal{A}'' &= \langle \widehat{a}^\dagger_{p_1}(t_1)\widehat{a}_{p_2}(t_2)\widehat{a}^\dagger_{q_1}(s_1)\widehat{a}_{q_2}(s_2)\rangle \\ &= \int d^{2M}\boldsymbol{\alpha}\,\mathrm{Tr}\Big[\widehat{a}^\dagger_{q_1}\breve{V}(s_1,t_2)\Big\{ \\ &\breve{V}(t_2,s_2)\Big\{\widehat{a}_{q_2}\breve{V}(s_2,t_1)\big\{P(\boldsymbol{\alpha},t_1)\widehat{\Lambda}_1(\boldsymbol{\alpha})\widehat{a}^\dagger_{p_1}\big\}\Big\}\widehat{a}_{p_2}\Big\}\Big]\end{aligned} \tag{71}$$

whose times satisfy (17), and $t_1 \leqslant s_2 \leqslant t_2 < s_1$ (for instance). The initial expansion of $\widehat{\rho}$ is made in the P representation, where $P(\boldsymbol{\alpha}) = W_1(\boldsymbol{\alpha})$ and $\widehat{\Lambda}_1(\boldsymbol{\alpha}) = |\boldsymbol{\alpha}\rangle\langle\boldsymbol{\alpha}|$. The first two operators $\widehat{a}^\dagger_{p_1}$, $\widehat{a}_{q_2}$, and first two $\breve{V}$ convert easily to phase-space variables via (5a) and (5d), giving

$$\begin{aligned}\mathcal{A}'' = \iiint d^{2M}\boldsymbol{\alpha}\,d^{2M}\underline{\boldsymbol{\alpha}}\,d^{2M}\underline{\underline{\boldsymbol{\alpha}}}\,\mathrm{Tr}\Big[\widehat{a}^\dagger_{q_1}\breve{V}(s_1,t_2)\Big\{ \\ \mathcal{P}_1(\boldsymbol{\alpha},t_2|\underline{\underline{\boldsymbol{\alpha}}},s_2)\mathcal{P}_1(\underline{\underline{\boldsymbol{\alpha}}},s_2|\underline{\boldsymbol{\alpha}},t_1)P(\underline{\boldsymbol{\alpha}},t_1)\,\underline{\alpha}_{q_2}\,\underline{\alpha}^*_{p_1}\widehat{\Lambda}_1(\boldsymbol{\alpha})\widehat{a}_{p_2}\Big\}\Big].\end{aligned} \tag{72}$$

Further work by this route is now closed because $\widehat{\Lambda}_1\widehat{a}_{p_2}$ involves (5c) and derivatives. Instead, another result that follows from from [19] allows us to convert kernels:

$$\begin{aligned}&\widehat{\Lambda}_s(\boldsymbol{\alpha}) \\ &= \left(\frac{2}{s-s_0}\right)^M \int \frac{d^{2M}\boldsymbol{\alpha}'}{\pi^M}\exp\left[-\frac{2|\boldsymbol{\alpha}'-\boldsymbol{\alpha}|^2}{s-s_0}\right]\widehat{\Lambda}_{s_0}(\boldsymbol{\alpha}').\end{aligned} \tag{73}$$

Taking $s = 1$ and $s_0 = -1$, to move to a Q representation kernel, one finds

$$\widehat{\Lambda}_1(\boldsymbol{\alpha}) = \int \frac{d^{2M}\boldsymbol{\zeta}}{\pi^M}\exp\left[-|\boldsymbol{\zeta}|^2\right]\widehat{\Lambda}_Q(\boldsymbol{\alpha}'). \tag{74}$$

where $\boldsymbol{\zeta} = \boldsymbol{\alpha}' - \boldsymbol{\alpha} = \{\zeta_j\}$ has exactly the properties of the noise in (68), and $\boldsymbol{\alpha}' = \boldsymbol{\alpha} + \boldsymbol{\zeta}$ is given by (69). After substituting (74) into (72), applying (56c) to $\widehat{\Lambda}_Q(\boldsymbol{\alpha}')\widehat{a}_{p_2}$, and defining the distribution

$$\begin{aligned}\widetilde{P}(\boldsymbol{\alpha}',t_2) = \alpha'_{p_2}\int \frac{d^{2M}\boldsymbol{\alpha}}{\pi^M}e^{-|\boldsymbol{\alpha}'-\boldsymbol{\alpha}|^2}\iint d^{2M}\underline{\boldsymbol{\alpha}}\,d^{2M}\underline{\underline{\boldsymbol{\alpha}}} \\ \mathcal{P}_1(\boldsymbol{\alpha},t_2|\underline{\underline{\boldsymbol{\alpha}}},s_2)\mathcal{P}_1(\underline{\underline{\boldsymbol{\alpha}}},s_2|\underline{\boldsymbol{\alpha}},t_1)P(\underline{\boldsymbol{\alpha}},t_1)\,\underline{\alpha}_{q_2}\,\underline{\alpha}^*_{p_1}.\end{aligned} \tag{75}$$

we have

$$\mathcal{A}'' = \int d^{2M}\boldsymbol{\alpha}'\,\mathrm{Tr}\left[\widehat{a}^\dagger_{q_1}\breve{V}(s_1,t_2)\Big\{\widetilde{P}(\boldsymbol{\alpha}',t_2)\,\widehat{\Lambda}_Q(\boldsymbol{\alpha}')\Big\}\right]. \tag{76}$$

Now using (27), and taking care with variable labels:

$$\begin{aligned}\mathcal{A}'' = \iint d^{2M}\boldsymbol{\alpha}'\,d^{2M}\underline{\boldsymbol{\alpha}}'\;\mathcal{P}_{-1}(\boldsymbol{\alpha}',s_1|\underline{\boldsymbol{\alpha}}',t_2)\widetilde{P}(\underline{\boldsymbol{\alpha}}',t_2) \\ \times\mathrm{Tr}\left[\widehat{a}^\dagger_{q_1}\widehat{\Lambda}_Q(\boldsymbol{\alpha}')\right].\end{aligned} \tag{77}$$

After the variable change caused by (27), now

$$\underline{\boldsymbol{\alpha}}' = \boldsymbol{\alpha} + \boldsymbol{\zeta}. \tag{78}$$

Notice also the -1 label on the latest propagator in (77), indicating that it is according to the Q representation equations in the time interval $(t_2, s_2]$. Finally, applying (56b), one arrives at:

$$\begin{aligned}\mathcal{A}'' = \int d^{2M}\underline{\boldsymbol{\alpha}}\,d^{2M}\underline{\underline{\boldsymbol{\alpha}}}\,d^{2M}\boldsymbol{\alpha}\,d^{2M}\boldsymbol{\zeta}\left(\frac{e^{-|\zeta|^2}}{\pi^M}\right)d^{2M}\boldsymbol{\alpha}' \\ \times\,\underline{\underline{\alpha}}_{q_2}\,\underline{\alpha}^*_{p_1}(\alpha_{p_2}+\zeta_{p_2})\alpha'^*_{q_1}\mathcal{P}_{-1}(\boldsymbol{\alpha}',s_1|\boldsymbol{\alpha}+\zeta,t_2) \\ \times\mathcal{P}_1(\boldsymbol{\alpha},t_2|\underline{\underline{\boldsymbol{\alpha}}},s_2)\mathcal{P}_1(\underline{\underline{\boldsymbol{\alpha}}},s_2|\underline{\boldsymbol{\alpha}},t_1)P(\underline{\boldsymbol{\alpha}},t_1).\end{aligned} \tag{79}$$

This encodes the following sequence of operations:

1. Start with initial samples $\underline{\boldsymbol{\alpha}}$ at t_1.
2. Propagate P representation equations to s_2 obtaining samples $\underline{\underline{\boldsymbol{\alpha}}}$.
3. Propagate P representation equations to t_2 obtaining samples $\boldsymbol{\alpha}$.
4. Add Gaussian noise as per (78), to get samples $\underline{\boldsymbol{\alpha}}'$.
5. Propagate Q representation equations to s_1 obtaining samples $\boldsymbol{\alpha}'$.

Along the way, samples are collected to use in the final stochastic average. The $\mathcal{P}_s$ factors in (79) together with the Gaussian factor in the top line form the joint probability $P(\boldsymbol{\alpha}', s_1; \underline{\boldsymbol{\alpha}}', t_2; \underline{\underline{\boldsymbol{\alpha}}}, s_2; \underline{\boldsymbol{\alpha}}, t_1)$. Therefore, the final estimator for the observable $\mathcal{A}''$ is

$$\begin{aligned}\mathcal{A}'' = \langle \widehat{a}^\dagger_{p_1}(t_1)\widehat{a}_{p_2}(t_2)\widehat{a}^\dagger_{q_1}(s_1)\widehat{a}_{q_2}(s_2)\rangle = \\ \langle \alpha^*_{p_1}(t_1)\alpha'_{p_2}(t_2)\alpha'^*_{q_1}(s_1)\alpha_{q_2}(s_2)\rangle_{\mathrm{stoch}}.\end{aligned} \tag{80}$$

Primed variables α' are samples of the Q distribution, while un-primed ones α are samples of the P distribution. This all matches intuitively with the evolution and the expectation that anti-normally ordered elements will use Q distribution samples and normally-ordered elements samples of the P distribution.

5.4 Most general ordering case

The widest generalisation of this procedure to other (time-ordered) cases is as follows: If there is an early time set of normally ordered operators, on either side

of the correlation, it can be dealt with by sampling the P distribution according to the replacements

$$\widehat{a}_j \to \alpha_j \qquad ; \qquad \widehat{a}_j^\dagger \to \alpha_j^*. \tag{81}$$

Once this avenue becomes exhausted, one adds noise via (69) to convert α's to Q distribution samples α'. If the remaining later time inner factors are anti-normally ordered, they can then be dealt with using the replacement

$$\widehat{a}_j \to \alpha'_j \qquad ; \qquad \widehat{a}_j^\dagger \to \alpha_j'^*. \tag{82}$$

The above covers both fully normal and fully anti-normal ordered products as special cases. On the other hand, the case of an early time anti-normally ordered block and a later time normally ordered block containing several times is not amenable to this approach because one cannot stochastically convert Q samples to P samples.

A large number of cases can also be reduced to a form amenable to this procedure by the use of the commutator $[\widehat{a},\widehat{a}^\dagger]=1$ for equal time factors. Also, simulations starting in a Wigner representation can be used for evaluation of outer symmetric ordered parts, and then a switch can be made to the Q representation via (70) to evaluate any remaining inner anti-normal ordered parts.

Order (number of operators)	1st order	2nd order	3rd order
Total permutations	**2**	**12**	**104**
single time correlations	2	4	8
multi-time accessible with P representation	–	4	22
additional accessible with Q representation	–	4	22
additional accessible with mixed order (Sec. 5.4)	–	–	22
Total doable	**2**	**12**	**74**
time ordered not doable	–	–	6
Not time ordered, not doable	–	–	24

Table 1: A tally of $\widehat{a}$, $\widehat{a}^\dagger$ product permutations that can/cannot be evaluated with the various approaches discussed. The general form considered is $\langle \widehat{A}(t_a)\widehat{B}(t_b)\widehat{C}(t_c)\rangle$, where $\widehat{A},\widehat{B},\widehat{C}$ can be either of $\widehat{a}$ or $\widehat{a}^\dagger$ (same mode), and the time arguments can take up to three distinct times $t_1 \le t_2 \le t_3$. Permutations with the same time topology (e.g. $\widehat{A}(t_1)\widehat{B}(t_1)\widehat{C}(t_2)$ and $\widehat{A}(t_2)\widehat{B}(t_2)\widehat{C}(t_3)$) are counted only once.

5.5 Correlation function coverage

Table 1 counts the number of distinct 1, 2, and 3 annihilation/creation operator products that can be evaluated using the various methodology described above. All one and two-factor combinations can be evaluated (though 4/12 of the latter require use of the Q representation). For third order correlations, almost all time-ordered cases can be evaluated (74 out of 80). The majority require use of the Q representation or a shift from a P to Q representation as described in Sec. 5.4 to work. There are 6 exceptions that cannot be evaluated: $\langle \widehat{a}^\dagger(t_2)\widehat{a}^\dagger(t_3)\widehat{a}^\dagger(t_1)\rangle$, $\langle \widehat{a}(t_2)\widehat{a}^\dagger(t_3)\widehat{a}(t_1)\rangle$, $\langle \widehat{a}(t_1)\widehat{a}(t_3)\widehat{a}(t_2)\rangle$, $\langle \widehat{a}(t_1)\widehat{a}^\dagger(t_3)\widehat{a}(t_2)\rangle$, $\langle \widehat{a}(t_3)\widehat{a}(t_2)\widehat{a}^\dagger(t_1)\rangle$, $\langle \widehat{a}^\dagger(t_3)\widehat{a}(t_2)\widehat{a}^\dagger(t_1)\rangle$, where $t_1 < t_2 < t_3$ is assumed. These all share the feature that the earliest factor already requires the Q representation, while the next operator in time requires the P representation to which one cannot return. There are also a number of correlations that are not time ordered, for which the earliest time t_1 is on the middle operator, and these are not possible to evaluate according to the schemes presented here.

The greatest interest in multi-time correlations usually concerns those involving two times (say $t=0$ and $t=\tau>0$). Examples are counting correlations like $\langle \widehat{a}^\dagger(0)\widehat{a}^\dagger(\tau)\widehat{a}(\tau)\widehat{a}(0)\rangle$, and pair correlations such as $\langle \widehat{a}^\dagger(0)\widehat{a}^\dagger(0)\widehat{a}(\tau)\widehat{a}(\tau)\rangle$. The case count for these is summarised by Table 2. A we can see, all 160 kinds of time ordered four-operator products of this form can be evaluated, including atypical combinations such as $\langle \widehat{a}(0)\widehat{a}^\dagger(\tau)\widehat{a}^\dagger(\tau)\widehat{a}(0)\rangle$, but very many require the Q representation. (72 out of the 160 accessible ones require the use of the mid-simulation switching to the Q representation described in Sec. 5.4). The only correlations that are inaccessible are the non time ordered ones such as e.g. $\langle \widehat{a}^\dagger(\tau)\widehat{a}^\dagger(0)\widehat{a}(0)\widehat{a}(\tau)\rangle$.

The change of distribution can introduce additional restrictions. In particular, Wigner and Q distributions have a tendency to involve higher order derivatives in the PDE (7) than P distributions, so that a standard diffusion process no longer captures the full quantum dynamics. An example are two-photon losses with operators $\widehat{R}=\widehat{a}^2$ for which P distributions produce only 2nd order derivatives but Q distributions 4th order terms, and Wigner distributions 3rd order ones. This precludes fully accurate calculation of correlation functions such as $\langle \widehat{a}^\dagger(0)\widehat{a}(t)\widehat{a}(t)\widehat{a}^\dagger(0)\rangle = \langle \alpha^*(0)\alpha'(t)\alpha'(t)\alpha'^*(0)\rangle_{\rm stoch}$ requiring Q evolution after the changeover, but not cases where the change to a Q distribution is only needed at the final time such as $\langle \widehat{a}^\dagger(0)\widehat{a}(t)\widehat{a}^\dagger(t)\widehat{a}(0)\rangle = \langle \alpha^*(0)\alpha'(t)\alpha'^*(t)\alpha(0)\rangle_{\rm stoch}$. Stochastic techniques for dealing with higher order PDE terms have been investigated [79, 80, 109, 117] particularly in [48] for doubled phase space, though attempts to date have shown strong time and stability limitations.

Order (number of operators)	2nd order	3rd order	4th order
Total permutations	**12**	**56**	**240**
single time correlations	4	8	16
multi-time accessible with P representation	4	14	36
additional accessible with Q representation	4	14	36
additional accessible with mixed order (Sec. 5.4)	–	12	72
Total doable	**12**	**48**	**160**
time ordered not doable	–	–	–
Not time ordered, not doable	–	8	80

Table 2: A tally of $\widehat{a}$, $\widehat{a}^\dagger$ products involving up to four operators, evaluated at one of two times. The general form considered is $\langle \widehat{A}(t_a)\widehat{B}(t_b)\widehat{C}(t_c)\widehat{D}(t_d)\rangle$, where $\widehat{A},\widehat{B},\widehat{C},\widehat{D}$ can be either of $\widehat{a}$ or $\widehat{a}^\dagger$ (same mode), and the time arguments can take up to two distinct times $t=0$ and $t=\tau>0$.

6 Q representations and s-ordering in doubled phase space

To use the mechanisms described in Sec. 5 in the doubled phase-space representations that give more complete coverage of quantum mechanics, we need also to consider the doubled phase space Q representation and how to switch to it from the positive-P.

6.1 Doubled phase space s-ordered representations

The s-ordered representations were first generalised to doubled phase space by de Oliveira [31]. Later studies [35, 71, 116] used a different normalisation that is closer to the original single-phase space formulation (52) of Cahill and Glauber [19]. It will also be used here. The explicit expansion of the density matrix was given in [35] as[3]:

$$\widehat{\rho} = \int d^{4M}\boldsymbol{\lambda}\, W_s^+(\boldsymbol{\lambda})\widehat{\Lambda}_s^+(\boldsymbol{\lambda}) \tag{83a}$$

$$\widehat{\Lambda}_s^+(\boldsymbol{\lambda}) = \prod_j \widehat{d}_j(\alpha_j,\beta_j)\widehat{T}_j(0,-s)\widehat{d}_j(-\alpha_j,-\beta_j), \tag{83b}$$

where the displacement-like operator $\widehat{d}$ is

$$\widehat{d}_j(\alpha_j,\beta_j) = e^{\alpha_j\widehat{a}_j^\dagger - \beta_j\widehat{a}_j} \quad ; \quad \widehat{d}_j(\alpha,\alpha^*) = \widehat{D}_j(\alpha), \tag{84}$$

obtained by the replacement $\alpha^* \to \beta$ in (52). To distinguish from single phase space, the superscript $^+$ is used where necessary. The usual properties $\mathrm{Tr}\left[\widehat{\Lambda}_s^+\right]=1$ and $\widehat{d}^{-1}(\alpha,\beta)=\widehat{d}(-\alpha,-\beta)$ continue to apply. The operator identities are now

$$\widehat{a}_j\widehat{\Lambda}_s^+ = \left[\alpha_j - \frac{1-s}{2}\frac{\partial}{\partial\beta_j}\right]\widehat{\Lambda}_s^+, \tag{85a}$$

$$\widehat{a}_j^\dagger\widehat{\Lambda}_s^+ = \left[\beta_j + \frac{1+s}{2}\frac{\partial}{\partial\alpha_j}\right]\widehat{\Lambda}_s^+, \tag{85b}$$

$$\widehat{\Lambda}_s^+\widehat{a}_j = \left[\alpha_j + \frac{1+s}{2}\frac{\partial}{\partial\beta_j}\right]\widehat{\Lambda}_s^+, \tag{85c}$$

$$\widehat{\Lambda}_s^+\widehat{a}_j^\dagger = \left[\beta_j - \frac{1-s}{2}\frac{\partial}{\partial\alpha_j}\right]\widehat{\Lambda}_s^+. \tag{85d}$$

The $s\to 1$ limit of all the above gives the positive-P representation, $s=0$ the doubled-Wigner representation of [71], and the limit $s\to -1$ a doubled phase space analogue to the Q representation ("doubled-Q"). Eqs. (85) are equivalent to the correspondences found in [31]. An advantage of the doubled-Q and doubled Wigner representations relative to their single-phase space analogues is that all 2nd order derivative terms in the PDE can be made positive-definite and converted fully to stochastic equations via the same analytic kernel trick as for the positive-P representation. For example, spontaneous emission in a Schwinger boson system need not be amputated like in [73] for the Wigner representation.

The kernel transform between different orderings in doubled phase-space is found to be

$$\widehat{\Lambda}_s^+(\boldsymbol{\alpha},\boldsymbol{\beta}) \tag{86}$$
$$= \left(\frac{2}{s-s_0}\right)^M \int \frac{d^{2M}\boldsymbol{\zeta}}{\pi^M}\exp\left[-\frac{2|\boldsymbol{\zeta}|^2}{s-s_0}\right]\widehat{\Lambda}_{s_0}^+(\boldsymbol{\alpha}+\boldsymbol{\zeta},\boldsymbol{\beta}+\boldsymbol{\zeta}^*),$$

which is easily verified with the help of

$$\widehat{T}_j(0,-s) = \frac{1}{\pi}\int d^2\gamma e^{-\frac{1}{2}s|\gamma|^2}\widehat{D}_j(\gamma) \tag{87}$$

from [19], the easy to show identities

$$\widehat{D}_j(\alpha)\widehat{D}_j(\gamma) = \widehat{D}_j(\alpha+\gamma)e^{\frac{1}{2}(\alpha\gamma^*-\alpha^*\gamma)} \tag{88a}$$

$$\widehat{d}_j(\alpha,\beta)\widehat{d}_j(\alpha',\beta') = \widehat{d}_j(\alpha+\alpha',\beta+\beta')e^{\frac{1}{2}(\alpha\beta'-\beta\alpha')}, \tag{88b}$$

and Gaussian integrals. The distribution transform

$$W_s^+(\boldsymbol{\alpha},\boldsymbol{\beta}) \tag{89}$$
$$= \left(\frac{2}{s_0-s}\right)^M \int \frac{d^{2M}\boldsymbol{\zeta}}{\pi^M}\exp\left[-\frac{2|\boldsymbol{\zeta}|^2}{s_0-s}\right]W_{s_0}^+(\boldsymbol{\alpha}+\boldsymbol{\zeta},\boldsymbol{\beta}+\boldsymbol{\zeta}^*).$$

is readily found by equating two (83a) expansions of $\widehat{\rho}$ which have different s, and applying (86) to the one with higher s ($=s_0$).

[3] In the supplemental material therein.

6.2 Non normally-ordered correlations in the positive-P representation

The ideas from Sec. 5 can be used to treat non normally-ordered correlations in the positive-P representation, which – unlike the Glauber-Sudarshan P – is applicable for all quantum states and systems. With the tools for the doubled s-ordered phase space described in Sec. 6.1, derivation of the expressions for mixed-time expectation values follows the same path as in Secs. 5.1 and 5.3, but some care needs to be taken to incorporate the doubled phase-space. We obtain that:

(1) To shift samples from a more to a less normally ordered doubled-phase space representation, one adds the following noise:

$$\alpha'_j = \alpha_j + \sqrt{\frac{s_0 - s}{2}}\ \zeta_j\ ;\ \beta'_j = \beta_j + \sqrt{\frac{s_0 - s}{2}}\ \zeta^*_j. \quad (90)$$

Notably – the same noise for α and β^*, which was not obvious *a priori*. The prefactor is 1 for positive-P to "doubled"-Q, and $1/\sqrt{2}$ for positive-P to doubled-Wigner.

(2) Anti-normal ordered mixed-time correlations are evaluated as

$$\langle \widehat{a}_{p_1}(t_1)\cdots\widehat{a}_{p_\mathcal{N}}(t_\mathcal{N})\widehat{a}^\dagger_{q_1}(s_1)\cdots\widehat{a}^\dagger_{q_\mathcal{M}}(s_\mathcal{M})\rangle$$
$$= \langle \alpha'_{p_1}(t_1)\cdots\alpha'_{p_\mathcal{N}}(t_\mathcal{N})\beta'_{q_1}(s_1)\cdots\beta'_{q_\mathcal{M}}(s_\mathcal{M})\rangle_{\rm stoch}. \quad (91)$$

where α' and β' are doubled-Q representation samples, possibly created via (90) (with $s_0 - s = 2$) from initial positive-P samples, and later evolved via the appropriate doubled-Q representation evolution equations.

(3) For mixed ordering, the procedure in Sec. 5.4 follows with the same structure, except that the correspondences are

$$\widehat{a}_j \to \alpha_j \quad ; \quad \widehat{a}^\dagger_j \to \beta_j. \quad (92)$$

in the positive-P and

$$\widehat{a}_j \to \alpha'_j \quad ; \quad \widehat{a}^\dagger_j \to \beta'_j. \quad (93)$$

in the doubled-Q. For example, the expression for the correlation $\mathcal{A}''$ (80) using samples starting in the positive-P is

$$\mathcal{A}'' = \langle \beta_{p_1}(t_1)\alpha'_{p_2}(t_2)\beta'_{q_1}(s_1)\alpha_{q_2}(s_2)\rangle_{\rm stoch} \quad (94)$$

(4) The correlation tallies of Sec. 5.5 apply without change to the doubled phase space representations.

7 Test example: unconventional photon blockade

7.1 The system

Consider the two-site Bose-Hubbard Hamiltonian

$$\widehat{H} = \sum_{j=1,2}\widehat{a}^\dagger_j\left[-\Delta + \frac{U}{2}\widehat{a}^\dagger_j\widehat{a}_j\right]\widehat{a}_j$$
$$+F\left[\widehat{a}^\dagger_1 + \widehat{a}_1\right] - J\left[\widehat{a}^\dagger_1\widehat{a}_2 + \widehat{a}^\dagger_2\widehat{a}_1\right] \quad (95)$$

with standard annihilation operators $\widehat{a}_j$ for modes j using units $\hbar = m = 1$. This describes two sites with (real) tunnelling J, local on-site interaction constant U, detuning Δ, and a coherent drive F (real) only on the first site. There is also a decay process with rate γ that is treated by describing the evolution of the system with the master equation

$$\frac{\partial\widehat{\rho}}{\partial t} = -i\left[\widehat{H},\widehat{\rho}\right] + \frac{\gamma\overline{N}}{2}\sum_j\left[2\widehat{a}^\dagger_j\widehat{\rho}\widehat{a}_j - \widehat{a}_j\widehat{a}^\dagger_j\widehat{\rho} - \widehat{\rho}^\dagger\widehat{a}_j\widehat{a}_j\right]$$
$$+\frac{\gamma(\overline{N}+1)}{2}\sum_j\left[2\widehat{a}_j\widehat{\rho}\widehat{a}^\dagger_j - \widehat{a}^\dagger_j\widehat{a}_j\widehat{\rho} - \widehat{\rho}\widehat{a}^\dagger_j\widehat{a}_j\right]. \quad (96)$$

To test the performance a bit more beyond the standard model, we have also addded a thermal bath with mean occupation $\overline{N}$. Such a system can be realised using e.g. micropillars [69, 123] or transmon qubits [72, 122]. The nontrivial feature here is a two-boson destructive interference effect between photons injected by the drive, and other photons that have been previously injected, tunnelled to site 2 and then back, returning with a relative phase of π [10]. The result of this is that in the steady state only single photons can be present at the driven site 1, providing possibly an avenue to create single-photon sources [96]. The lack of double occupation is evidenced in a single-time two body correlation function $g_{11} = \langle\widehat{a}^{\dagger 2}_1\widehat{a}^2_1\rangle/\langle\widehat{a}^\dagger_1\widehat{a}_1\rangle^2$, which is very close to zero. However, for practical application, it is of particular interest to find out how large a time mismatch between measured photons can be accommodated without significantly increasing $g^{(2)}_{11}$ from this low level. If it is too short, then the single-photon source will have a too short active time for practical applications. Therefore the correlation function of particular interest is

$$g_{11}(\tau) = \frac{\langle\widehat{a}^\dagger_1(t)\widehat{a}^\dagger_1(t+\tau)\widehat{a}_1(t+\tau)\widehat{a}_1(t)\rangle}{n^2_1} \quad (97)$$

in the stationary state, with delay time τ. The mean occupation is $n_1 = \langle\widehat{a}^\dagger_1\widehat{a}_1\rangle$.

The Ito stochastic evolution equations in the positive-P ($s = 1$) and doubled-Q ($s = -1$) representations are

$$\frac{d\alpha_j}{dt} = \left[-iU(\alpha_j\beta_j + s - 1) - \frac{\gamma}{2} + \sqrt{-isU}\,\xi_j(t)\right]\alpha_j - iF_j$$
$$-i\sum_k H^{\rm sp}_{jk}\alpha_k + \sqrt{\gamma\left(\overline{N} + \tfrac{1-s}{2}\right)}\,\eta_j(t) \qquad (98a)$$

$$\frac{d\beta_j}{dt} = \left[iU(\alpha_j\beta_j + s - 1) - \frac{\gamma}{2} + \sqrt{isU}\,\widetilde{\xi}_j(t)\right]\beta_j + iF_j$$
$$+i\sum_k H^{\rm sp}_{jk}\beta_k + \sqrt{\gamma\left(\overline{N} + \tfrac{1-s}{2}\right)}\,\eta^*_j(t). \qquad (98b)$$

These were derived in [45] for the positive-P. Here the matrix elements of the one-particle Hamiltonian are $H^{\rm sp}_{jj} = -\Delta$, $H^{\rm sp}_{12} = H_{21} = -J$, the drives are $F_1 = F$, $F_2 = 0$, while ξ_j and $\widetilde{\xi}_j$ are delta-correlated independent white real noises with variance

$$\langle \xi_j(t)\xi_{j'}(t')\rangle = \delta_{jj'}\delta(t-t') \qquad (99)$$

and η_j are similarly correlated independent complex noises:

$$\langle \eta_j(t)\eta^*_{j'}(t')\rangle = \delta_{jj'}\delta(t-t'); \qquad \langle \eta_j(t)\eta_{j'}(t')\rangle = 0. \qquad (100)$$

Appendix A.3 gives some detail on generation of the noise. In some cases, calculations with these stochastic equations can already be faster than brute force calculations directly with the density matrix $\widehat{\rho}$ in a suitably truncated number state basis. For large systems, they are the only tractable way to access full quantum mechanics. Appendix A gives details of an integration algorithm that is robust to the multiplicative noise appearing in (98), and was used for the simulations reported here and elsewhere [35, 36, 41–45, 82, 107, 120, 134].

7.2 Two-time photon-photon correlations

Consider first the strong antibunching parameters studied in [10] and [45]: $U = 0.0856$, $J = 3$, $\Delta = -0.275$, $\gamma = 1$, $F = 0.01$. We will study the correlations primarily in the stationary state. To this end, a positive-P simulation is initialised in the vacuum $\boldsymbol{\alpha} = \boldsymbol{\beta} = 0$, and evolved up to $t = 30$. The stationary state is attained after $t \gtrsim 15$, and we calculate multi time correlation functions from times $t_0 = 20$ to $t_0 + \tau$ using the available samples. ($\mathcal{S} = 2^{16}$ in all cases). Uncertainty in predictions is calculated using sub-ensemble averaging, as explained in Appendix A.4. These errors are shown as triple lines in all the plots.

The two-time photon-photon correlations between one photon measured at site 1 at time t_0 and the other at site j after a delay time of τ are

$$g_{1,j}(\tau) = \frac{\langle \widehat{a}^\dagger_1(t_0)\widehat{a}^\dagger_j(t_0+\tau)\widehat{a}_j(t_0+\tau)\widehat{a}_1(t_0)\rangle}{n_1(t_0)n_j(t_0+\tau)}, \qquad (101)$$

where $n_j(t) = \langle \widehat{a}^\dagger(t)\widehat{a}(t)\rangle = {\rm Re}\langle\alpha_j(t)\beta_j(t)\rangle_{\rm stoch}$ is the mean occupation of site j. In the positive-P representation the correlation (101) is calculated via

$$g_{1,j}(\tau) = \frac{{\rm Re}\,\langle\alpha_1(t_0)\beta_1(t_0)\alpha_j(t_0+\tau)\beta_j(t_0+\tau)\rangle_{\rm stoch}}{n_1(t_0)n_j(t_0+\tau)}. \qquad (102)$$

We can take the real parts above, because the imaginary parts must converge to zero in the $\mathcal{S}\to\infty$ limit. This behaviour is verified in the simulations.

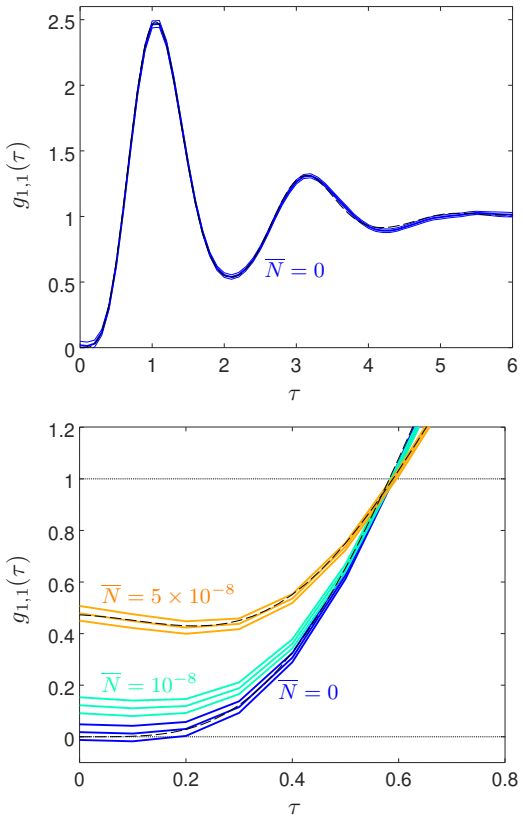


Figure 1: Time duration of antibunching in the unconventional photon blockade system, $F = 0.01$. Top: clean system ($\overline{N} = 0$), strong antibunching. Bottom: degradation with background thermal intensity $\overline{N} > 0$. Black dashed lines: direct solution of the master equation. Triple lines show 1σ statistical uncertainty.

Fig. 1 (top) shows the multi-time local photon correlation (101) at site 1 (i.e. $j = 1$) for the clean case ($\overline{N} = 0$), and verifies that the result perfectly matches the exact brute force solution. The desired anti-correlation dip is seen around $\tau = 0$, along with characteristic oscillations out to delay times of about $\tau = 5$. The bottom panel shows how the anti-correlation dip degrades when the system is linked to a particle reservoir (growing $\overline{N}$). Notably the dip timescale does not change appreciably as the minimum correlation rises. A 10% remnant correlation which might still be acceptable

for applications is found when $\overline{N} = 10^{-8} = 0.026 n_1$. This sets a limit on how much background photon reservoir is acceptable.

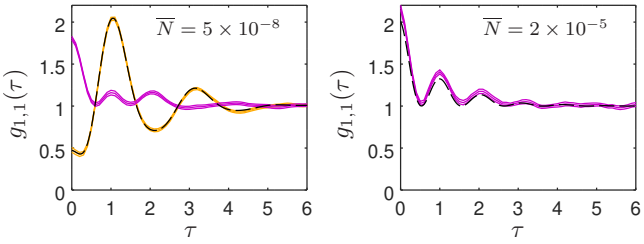


Figure 2: Breakdown of the Glauber-Sudarshan P representation: shown in pink; Positive-P simulation: yellow; exact: black dashed. $F = 0.01$.

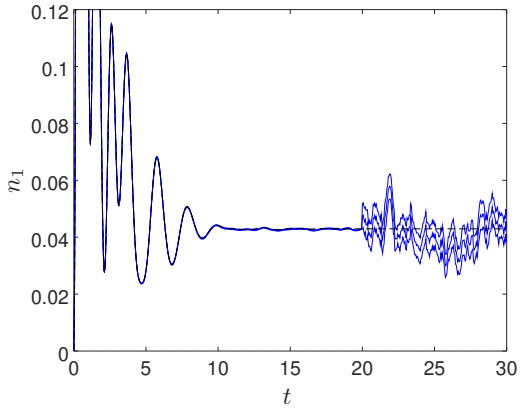


Figure 3: Estimation in positive-P and doubled-Q simulations: occupation of mode 1, when $F = 3$, after switching from the positive-P to the doubled-Q representation at $t = t_0 = 20$.

7.3 Breakdown of the Glauber-Sudarshan P

This system also shows the breakdown of the single-phase-space P representation very clearly. The evolution equation is (98a) with $s = 1$, but it is a correct representation of the quantum FPE (8) only when the diffusion matrix $D_{\mu\nu}$ in the FPE has all nonnegative eigenvalues [62]. Here, the diffusion matrix for real, imaginary parts of $\alpha_j = \alpha_{jr} + i\alpha_{ji}$ has elements $D_{jr,jr} = \frac{U}{2}\mathrm{Im}(\alpha_j^2) + \frac{\gamma\overline{N}}{2}$, $D_{ji,ji} = -\frac{U}{2}\mathrm{Im}(\alpha_j^2) + \frac{\gamma\overline{N}}{2}$, $D_{jr,ji} = D_{ji,jr} = -\frac{U}{2}\mathrm{Re}(\alpha_j^2)$. with eigenvalues $\lambda_{j,\pm} = \frac{\gamma\overline{N}}{2} \pm \frac{U}{2}|\alpha_j|^2$. These only become non-negative once $\gamma\overline{N} > U|\alpha_j|^2$, i.e. $\gamma\overline{N} \gtrsim U n_j$. The question then is: for what parameters does the evolution remain well described? When $\overline{N} = 0$ The anti-bunched mode has mean occupation $n_1 = 3.87 \times 10^{-7}$, naively suggesting $\overline{N} \sim 5 \times 10^{-8} = 1.5 U n_1/\gamma$ to already be a value for which the description is good. However, we can see in Fig. 2 that it does not give correct results at all. This is because the problem lies in the nr. 2 mode with $n_2 = 1.07 \times 10^{-5}$. Taking a far larger $\overline{N} = 2 \times 10^{-5}$ (in which case $\gamma\overline{N} \sim 10 U n_1, 7 U n_2$) gives almost correct results with the Glauber-Sudarshan P (though still not fully), but of course antibunching in mode 1 is long gone for such a relatively high thermal noise level.

This is an indication that skimping on full quantum effects by trying approximate semiclassical methods is not a good strategy for this kind of system.

7.4 Differently ordered correlations

To test how the prescriptions developed in Secs. 4.1 and 5 work, we use a different driving, $F = 3$, which generates larger occupations (in the stationary state $n_1 \approx 0.043$ and $n_2 \approx 0.98$) and as a result more interesting anti-normal and mixed-order correlations. The doubled-Q simulations are also too noisy to get useful predictions for the parameters in Fig. 1 because Q distributions have a width of $\mathcal{O}(1)$ even in vacuum. This is a certain limitation to the Q distribution approach. The difference in sampling accuracy can be nicely seen in Fig. 3 which shows the mean and uncertainty of n_1 during the simulation used to generate Figs. 4-5. The samples are switched from positive-P to doubled-Q at $t = t_0 = 20$.

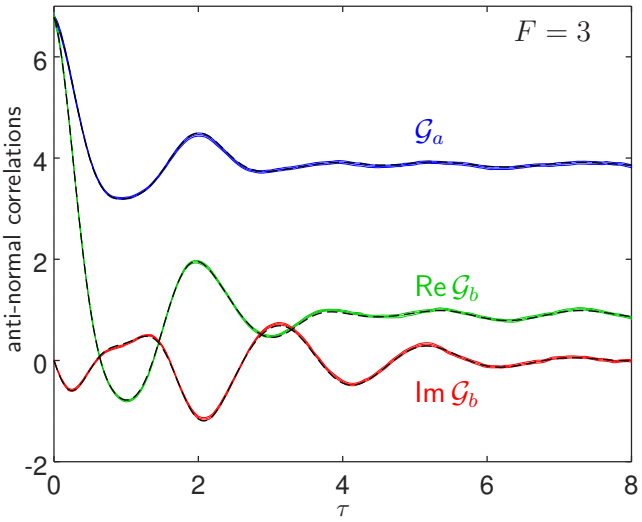


Figure 4: Anti-normal ordered moments. Strongly pumped case ($F_1 = 3$), mode 2. Shown are $\mathcal{G}_a$ and the real and imaginary parts of $\mathcal{G}_b$ as per (103). Exact results: dashed black.

Arguably the primary practical interest lies in cases with four factors and two times – corresponding roughly to either detection of single particles at two times, or creation and destruction of pairs. Fig. 4 shows the simulation of some anti-normally ordered correlations of this kind (not normalised), evaluated using the doubled-Q representation:

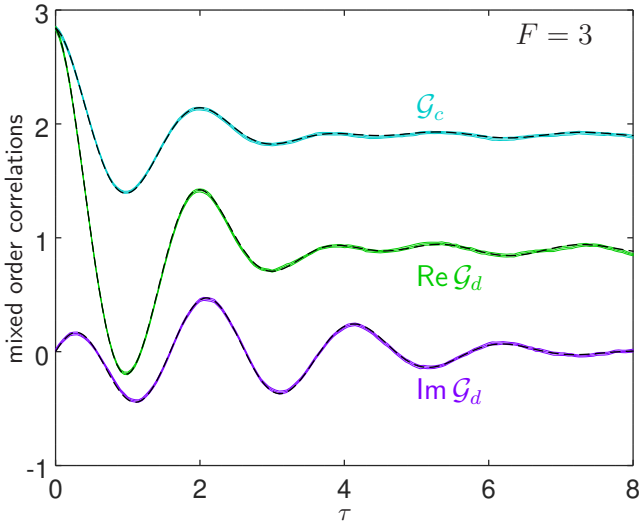


Figure 5: Moments that are neither normal nor anti-normal. $F = 3$ like in Fig. 4. Shown are $\mathcal{G}_c$ and the real and imaginary parts of $\mathcal{G}_d$ as per (104). Exact results: dashed black lines.

$$\begin{aligned}\mathcal{G}_a &= \langle \widehat{a}_2(t_0)\widehat{a}_2(t_0+\tau)\widehat{a}_2^\dagger(t_0+\tau)\widehat{a}_2^\dagger(t_0)\rangle \\ &= \mathrm{Re}\langle \alpha_2'(t_0)\alpha_2'(t_0+\tau)\beta_2'(t_0+\tau)\beta_2'(t_0)\rangle_{\mathrm{stoch}} \qquad (103)\\ \mathcal{G}_b &= \langle \widehat{a}_2(t_0+\tau)^2[\widehat{a}_2^\dagger(t_0)]^2\rangle = \langle \alpha_2'(t_0+\tau)^2\beta_2'(t_0)^2\rangle_{\mathrm{stoch}}\end{aligned}$$

The latter $\mathcal{G}_b$ is an anomalous correlation that has both real and imaginary components. Similarly, Fig. 5 shows simulations of a number of mixed-order correlations which absolutely require a swapping from positive-P to doubled-Q representation using the procedure of Sec. 5.4:

$$\begin{aligned}\mathcal{G}_c &= \langle \widehat{a}_2(t_0+\tau)\widehat{a}_2^\dagger(t_0+\tau)\widehat{a}_2^\dagger(t_0)\widehat{a}_2(t_0)\rangle \\ &= \mathrm{Re}\langle \alpha_2'(t_0+\tau)\beta_2'(t_0+\tau)\beta_2'(t_0)\alpha_2(t_0)\rangle_{\mathrm{stoch}} \\ \mathcal{G}_d &= \langle \widehat{a}_2(t_0)[\widehat{a}_2^\dagger(t_0+\tau)]^2\widehat{a}_2(t_0)\rangle \\ &= \langle \alpha_2'(t_0)\beta_2'(t_0+\tau)^2\alpha_2(t_0)\rangle_{\mathrm{stoch}} \qquad (104)\end{aligned}$$

In all cases, primed variables are evaluated in the doubled-Q representation, un-primed in the positive-P.

Notably, in both figures the stochastic simulations perfectly and very accurately agree with brute force calculations using the density matrix. This is despite the regime being one which is very poorly treated by approximate semiclassical methods (occupations are $\mathcal{O}(1)$ or smaller). This is strong evidence that the intuitive expressions and approach laid out in the previous sections is appropriate.

7.5 Correlation dynamics in the stationary state

As a larger-sized example, consider the same Hamiltonian and master equation as (95) and (96) (take $\overline{N} = 0$), but with a longer chain of 32 sites, which is already beyond or at the limit of the capabilities of alternative methods such as brute force or corner space renormalisation [24, 59]. The tunnelling term in (95) now becomes $-J\sum_{j=1}^{31}\left[\widehat{a}_j^\dagger\widehat{a}_{j+1} + \widehat{a}_{j+1}^\dagger\widehat{a}_j\right]$, and a driving of $F = 3$ remains only at the $j = 1$ site. While the stationary state does not show any time-dependent change in expectation values, we should expect to still see signatures of transport in its multi-time correlations as a function of distance and delay time if the method is good.

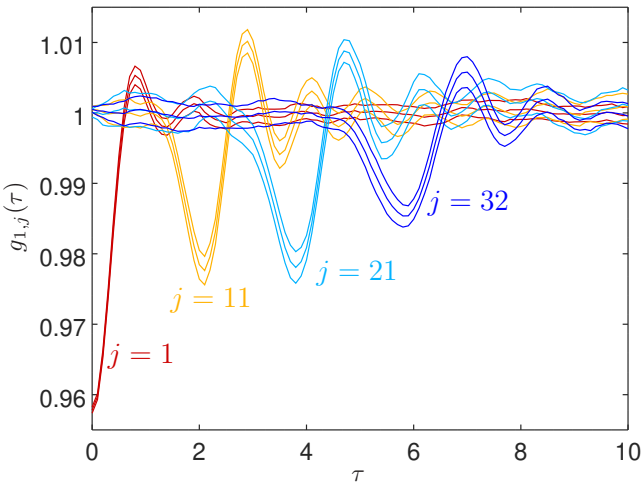


Figure 6: Spreading of correlations in a 32 site chain, in the stationary state. $F = 3$. The correlation is given by (101).

Fig. 6 shows such a calculation in the 32 site system, plotting the normalised photon-photon correlation $g_{1,j}(\tau)$ with spatial separation $j - 1$ and delay time τ, as defined in (101). The correlations are evaluated from $t_0 = 20$. Despite this being the stationary state, a very clear anti-correlation signal can be seen moving steadily with delay time. Its speed is approximately $2J$, twice the tunnelling rate. Correlation waves often travel at twice the characteristic speed for single particles [25, 97, 114], so this is not unexpected. However, the speed is clearly not related to the superfluid speed of sound, here $\sim \sqrt{Un_j}$, which is far lower.

8 Summary

The known framework for evaluation of multi-time observables from the work of Gardiner in the P representation [62] has been extended here to include firstly: the much more widely applicable positive-P representation (39); Secondly the Q (65), doubled-Q and other single and double phase space s-ordered representations; Thirdly: other orderings such as anti-normal and mixed-ordered observable products (Sec. 5, and especially (80) and the algorithm of Sec. 5.4). These results allow the

evaluation of a very wide range of quantum multi-time observables in bosonic systems (classified in Tables. 1-2) in a way that contains the full quantum mechanics, and is scalable to large systems. Systems with localised interactions require computational effort proportional to M or $M \log M$ with the number of modes or sites, M.

While out-of-time correlations (OTOCs) are not directly accessible through the mechanism outlined here, time reversal schemes like those used in experiment [63] or theory [15, 46, 133] could be attempted by changing the signs of constants in the equation of motion. When combined with the techniques developed here, this would give access to a wide range of information about quantum chaos [15, 60, 98], many body localisation [56, 70], and quantum phase transitions [124] in larger systems than were accessible to date [15, 63].

Along the way, a number of additional results were obtained regarding conversion formulae between different orderings in the doubled-phase space representations ((86) and (89)) and their stochastic samples (90). A clear case of the breakdown of the Glauber-Sudarshan P representation was seen in Fig. 2. Also, in Sec. 7 some results regarding the correlation functions (Figs. 4 and 5), susceptibility to background thermal density (Fig. 1) and signal speed (Fig. 6) in the unconventional photon blockade system were obtained.

Finally, Appendix A details a convenient algorithm for simulation of phase-space stochastic equations, an item that has been hard to find in the literature in the past.

Acknowledgments

I am grateful to Michał Matuszewski, Marzena Szymańska, and Alex Ferrier for discussions on topics leading to this paper, and to Wouter Vestraelen for discussions of numerics. This research was supported by the National Science Centre (Poland) grant No. 2018/31/B/ST2/01871.

A Numerical techniques for stochastic simulation of phase-space trajectories

This appendix details how the stochastic equations for the examples in Sec. 7 were integrated, and describes a robust and general algorithm that is particularly applicable to stochastic trajectories generated by phase-space descriptions of quantum systems. The bulk of the method is based on the semi-implicit midstep algorithm described in [51, 140], adding some modified propagators as per [44] which allow for more efficient treatment of exponential and dominant deterministic processes. Some practical elements that are usually skipped over in the literature are also pointed out. Example textbooks for the broad topic of stochastic integration include [76, 87].

A.1 Integration algorithm

Let us introduce the following notation. The Ito stochastic equations for a set of variables $\vec{v}$ with elements v_j indexed by j will be written

$$\frac{dv_j}{dt} = \mathcal{D}_j(\vec{v},t) = A_j(\vec{v},t) + X_j(\vec{v},t) \tag{105}$$

where X_j are noise terms with zero mean $\langle X_j\rangle_{\text{stoch}} = 0$, whereas A_j are deterministic "drift terms" that contain no explicit noise contribution, apart from the statistical spread of the variables v_j themselves. At the level of the Ito equations (105) we also require that the noise is not correlated in time $\langle X_j(t)X_{j'}(t')\rangle_{\text{stoch}} \propto \delta(t-t')$, i.e. proportional to Wiener increments. For example, in (98):

$$X_{\alpha_j} = \alpha_j\sqrt{-isU}\,\xi_j + \sqrt{\gamma\left(\overline{N}+\frac{1-s}{2}\right)}\,\eta_j, \tag{106a}$$

$$X_{\beta_j} = \beta_j\sqrt{isU}\,\widetilde{\xi}_j + \sqrt{\gamma\left(\overline{N}+\frac{1-s}{2}\right)}\,\eta_j^*. \tag{106b}$$

For various reasons, the standard mathematical environments and numerical packages tend not to perform well when integrating stochastic equations[4], especially ones that contain variable-dependent diffusion coefficients such as in (106) or the prototypical Kubo oscillator [90] with multiplicative noise. Phase space methods that treat the full quantum dynamics also typically contain such terms. Once one leaves the simplest Ito-Euler algorithm which requires very small step sizes, two of the recurring issues are that advanced integration algorithms usually assume sufficiently continuous derivatives (completely violated by white noise) or try to adapt the timestep in real time (which can introduce systematic errors when noise is involved). A third difficulty is the need for autocorrelation corrections (seen Sec. A.2) which become much more difficult to derive as the complexity of the algorithm grows.

The semi-implicit midpoint approach [47, 126] has been shown to be robust against spurious numerical instability as carefully analysed in [51, 140], but remains simple enough for any autocorrelation corrections to be readily calculated.

Suppose we are to advance time by Δt, starting from variables $v_j^{(0)}$ at time t to v_j' at $t+\Delta t$. Define a constituent substep or propagator that advances times by τ

[4] A notable exception is the XMDS package [33].

and variables to $v_j^{\rm step}\left[\vec{v}_j^{(0)}, \mathcal{D}(\vec{v}^{(0)},t),\tau\right]$ which depends in order on the starting variables, the form of the derivative, and the timestep τ. The simplest choice for this propagator is the Ito-Euler form

$$v_j^{\rm step}\left[v_j^{(0)}, \mathcal{D}(\vec{v}^{(0)},t),\tau\right] = v_j^{(0)} + \mathcal{D}(\vec{v}^{(0)},t)\,\tau \quad (107)$$

which just uses the values at the beginning of the step for evaluating the derivative, as per the definition of Ito stochastic calculus.

The semi-implicit midpoint algorithm can be viewed as a container procedure that calculates the final variables v_j' via a series of iterations [140]

$$\begin{aligned} v_j^{(1)} &= v_j^{\rm step}\left[v_j^{(0)}, \mathcal{D}(\vec{v}^{(0)},t),\Delta t/2\right], \\ v_j^{(2)} &= v_j^{\rm step}\left[v_j^{(0)}, \mathcal{D}(\vec{v}^{(1)},t),\Delta t/2\right], \\ &\cdots \\ v_j^{(n)} &= v_j^{\rm step}\left[v_j^{(0)}, \mathcal{D}(\vec{v}^{(n-1)},t),\Delta t/2\right], \end{aligned} \quad (108)$$

$$v_j'(t+\Delta t) = v_j^{\rm step}\left[v_j^{(0)}, \mathcal{D}(\vec{v}^{(n)},t+\Delta t/2),\Delta t\right]. \quad (109)$$

The numbered iterations always start from the initial point, but iteratively find a self-consistent estimate of the midpoint value of the derivatives. The last iteration (109) uses this midpoint value and midstep time to make the final advancement of the variables. Usually, a single midpoint iteration (i.e. $n = 1$) is sufficient. When using the basic Ito-Euler propagator (107) at time argument $t+\Delta t/2$ in (109), the final step is accurate to $\mathcal{O}(\Delta t^2)$ in the deterministic parts A_j, and the step's mean to order $\mathcal{O}(\Delta t)$ in the noise terms X_j [51], provided the autocorrelation correction is incorporated into $v_j^{\rm step}$, as explained in Sec. A.2. This is so-called "weak" stochastic convergence to $\mathcal{O}(\Delta t)$ in the terminology of [51] because the accuracy for single trajectories is $\mathcal{O}(\sqrt{\Delta t})$. "Strong" stochastic convergence to $\mathcal{O}(\Delta t)$ for single trajectories requires a more involved and more inconvenient autocorrelation correction than that presented in Sec. A.2. Nevertheless, the "weak" level of accuracy in the noise term is actually quite high already. For example, even 4th or 9th order Runge-Kutta implementations made available are generally only accurate to $\mathcal{O}(\sqrt{\Delta t})$ in this regard [33].

Moreover, in practice, one can often easily but substantially improve on the Euler step (107). For example, if Δ, γ, or U are large in (98), the evolution is primarily exponential. Another typical case is in continuum models when the kinetic energy or external potential energy contributions are dominant and trivial to integrate [44]. A pragmatic and flexible propagator choice is to separate the evolution into parts that will be treated exponentially (E), strictly linearly (L) and the rest (R):

$$\mathcal{D}_j(\vec{v}) = \mathcal{D}_j^E(\vec{v})\,v_j + \mathcal{D}_j^R(\vec{v}) + \mathcal{D}_j^L(\vec{v}), \quad (110)$$

and solve the equation for the E and R parts

$$\frac{dv_j}{d\tau} = \mathcal{D}_j^E\,v_j + \mathcal{D}_j^R \quad (111)$$

as if the coefficients were constant [44]. This gives the full propagator

$$\begin{aligned} &v_j^{\rm step}\left[v_j^{(0)}, \mathcal{D}(\vec{v}^{(0)},t),\tau\right] = \\ &\quad v_j^{(0)}\,e^{\tau\,\mathcal{D}_j^E(\vec{v}^{(0)},t)} + \left(e^{\tau\,\mathcal{D}_j^E(\vec{v}^{(0)},t)} - 1\right)\frac{\mathcal{D}_j^R(\vec{v}^{(0)},t)}{\mathcal{D}_j^E(\vec{v}^{(0)},t)} \\ &\quad + \mathcal{D}_j^L(\vec{v}^{(0)},t)\,\tau. \end{aligned} \quad (112)$$

Then, the leading processes are often integrated exactly, with only higher order corrections needed to be worked on by the midpoint algorithm. This is particularly efficient when the stochastic terms are a perturbation on the dominant exponential deterministic evolution. It is usually optimal to place all non-exponential parts into the "R" part, but some special cases can require avoidance of the nonlinear solution [44]. Both A drift and X noise parts can enter the coefficients as one chooses.

In the case of the calculations in this paper using (98),

$$\begin{aligned} \mathcal{D}_{\alpha_j}^E &= -iU(\alpha_j\beta_j + s - 1) - \frac{\gamma}{2} + \sqrt{-isU}\,\xi_j - iH_{jj}^{\rm sp} + C_{\alpha_j}^E, \\ \mathcal{D}_{\alpha_j}^R &= -iF_j - i\sum_{k\neq j} H_{jk}^{\rm sp}\alpha_k + \sqrt{\gamma\left(\overline{N} + \frac{1-s}{2}\right)}\,\eta_j, \\ \mathcal{D}_{\beta_j}^E &= iU(\alpha_j\beta_j + s - 1) - \frac{\gamma}{2} + \sqrt{isU}\,\widetilde{\xi}_j + iH_{jj}^{\rm sp} + C_{\beta_j}^E, \\ \mathcal{D}_{\beta_j}^R &= iF_j + i\sum_{k\neq j} H_{jk}^{\rm sp}\beta_k + \sqrt{\gamma\left(\overline{N} + \frac{1-s}{2}\right)}\,\eta_j^*, \end{aligned} \quad (113)$$

and $\mathcal{D}_j^L = 0$ were used for the propagator (112) and combined with a single iteration ($n = 1$) of the midpoint algorithm (108). Note the presence of the autocorrelation corrections

$$C_{\alpha_j}^E = \frac{isU}{2} \quad (114a)$$

$$C_{\beta_j}^E = -\frac{isU}{2} \quad (114b)$$

as explained in Sec. A.2.

Importantly – the form of the corrections (114) above arises when the noises ξ, η etc. appearing in the X_j are calculated just once at the beginning of the entire procedure for making the full Δt step. Other noise input can change the expressions (114).

The actual timestep Δt that must be used is constrained by the need for the coefficients $\mathcal{D}_j$ to change little over a single timestep Δt. A good practical rule of

thumb is to require

$$\frac{\left|\mathcal{D}^{(\nu)}(\vec{v},t)\,\Delta t\right|}{\left|v_j^{(0)}\right|} \lesssim 0.1, \tag{115}$$

for each term $\mathcal{D}^{(\nu)}$ in $\mathcal{D}=\sum_\nu \mathcal{D}^{(\nu)}$. One caveat is that one should take care not to estimate $\mathcal{D}(\vec{v}^{\,(0)},t)$ on the run using noise or even variable values from individual trajectories. Doing so can, and often does, introduce autocorrelations between noise values and time step lengths, leading to systematic errors. For treating noise terms, it is useful to use the RMS estimate $X_j \approx \sqrt{\langle |X_j|^2\rangle} \propto \sqrt{\Delta t}$ based on expected mean variable values $\langle v_j\rangle$ for timestep estimates.

Finally, for completeness and general applicability beyond the examples of Sec. 7, it can be advantageous to treat widely differing processes using a split-step approach [140]. In particular, the treatment of kinetic energy and tunnelling is much bettered for many-mode systems. A split step allows to take advantage of the fact that kinetic energy and tunnelling are diagonal in k-space and can be done exactly there. k-space is reached using a discrete Fast Fourier Transform that has computational cost of only $M\log M$ for an M-site system [61]. The split-step is applied in three parts:
(i) First evolve terms diagonal in k-space for $\Delta t/2$;
(ii) then change variables to x-space and evolve the remaining terms there for Δt;
(iii) finally return to k-space for another k-space evolution of $\Delta t/2$.

For cases like (98) in which the main mean-field evolution has a Gross-Pitaevskii form, the split step method is symplectic (conserves energy) and has been shown to have an accuracy of $\mathcal{O}(\Delta t)^2$ for the long time solution [77] provided that the latest available copy of the field is input as $\vec{v}^{\,(0)}$ after each Fourier transform [57]. Within each k- or x-space split step, the midpoint method (108) can employed if the coefficients $\mathcal{D}$ of the substep are variable-dependent, or otherwise if the coefficients are constant just a plain propagator substep (112) is done. Thus, one has the split-step algorithm as a container for midpoint iterations, which themselves are containers for the base propagators. Long-range interactions (eg. dipole-dipole) can also often be treated efficiently through Fourier transforms [144].

Sumarizing, the algorithm used for the simulations of Sec. 7 consists of (108), (109), (112)–(114).

A.2 Timestep autocorrelation correction

Realisations of Ito stochastic equations (105) must at the least produce the required average and noise variance to lowest order. That is, writing

$$\Delta v_j = v_j'(t+\Delta t) - v_j^{(0)}, \tag{116}$$

one needs

$$\begin{aligned}\langle \Delta v_j\rangle_{\rm stoch} &= \Big\langle A_j(\vec{v}^{\,(0)})\Delta t\Big\rangle_{\rm stoch} + \mathcal{O}(\Delta t)^{3/2}\\ \langle \Delta v_j \Delta v_k\rangle_{\rm stoch} &= \Big\langle X_j(\vec{v}^{\,(0)})X_k(\vec{v}^{\,(0)})\Delta t^2\Big\rangle_{\rm stoch} + \mathcal{O}(\Delta t)^{3/2}.\end{aligned} \tag{117}$$

In orders of Δt, the drift is $A_j\Delta t\sim\mathcal{O}(\Delta t)$ and the noise $X_j\Delta t\sim\mathcal{O}(\sqrt{\Delta t})$. The time-dependence of coefficients A and X does not enter at this order of Δt. A simple Ito-Euler timestep $v_j^{(0)}\to v_j^{(0)}+A_j(\vec{v}^{\,(0)})\,\Delta t + X_j(\vec{v}^{\,(0)})\,\Delta t$ meets both conditions (117).

However, the midstep algorithm with an Ito-Euler propagator (107) can introduce an extra correlation of order Δt by virtue of using the same noise for both the halfstep of $\Delta t/2$ and then for the final full step. The first halfstep advance using (107) produces

$$\begin{aligned}\Delta v_j^{(1)} = v_j^{(1)} - v_j^{(0)} &= A_j(\vec{v}^{\,(0)})\frac{\Delta t}{2} + X_j(\vec{v}^{\,(0)})\,\frac{\Delta t}{2},\\ &\sim \mathcal{O}(\sqrt{\Delta t})\end{aligned} \tag{118}$$

Note that the X_j themselves are $\mathcal{O}(\frac{1}{\sqrt{\Delta t}})$, which is important below. The next step in (108) involves coefficients $A_j(\vec{v}^{\,(1)})$ and $X_j(\vec{v}^{\,(1)})$. Taylor expanding around $\vec{v}^{\,(0)}$,

$$X_j(\vec{v}^{\,(1)}) = X_j(\vec{v}^{\,(0)}) + \sum_k \frac{dX_j}{dv_k}(\vec{v}^{\,(0)})\Delta v_k^{(1)} + \mathcal{O}(\sqrt{\Delta t}), \tag{119}$$

and analogously for A_j. Using (118) and discarding terms of subleading order $\mathcal{O}(\sqrt{\Delta t})$ in the new coefficients one finds

$$\begin{aligned}X_j(\vec{v}^{\,(1)}) &= X_j(\vec{v}^{\,(0)})\\ &\quad+\sum_k \frac{dX_j}{dv_k}(\vec{v}^{\,(0)})\,X_j(\vec{v}^{\,(0)})\frac{\Delta t}{2} + \mathcal{O}(\sqrt{\Delta t}),\\ A_j(\vec{v}^{\,(1)}) &= A_j(\vec{v}^{\,(0)}) + \mathcal{O}(\sqrt{\Delta t}).\end{aligned} \tag{120}$$

Notice the appearance of a term in $X_j(\vec{v}^{\,(1)})$ of the same order as the original coefficients $X_j(\vec{v}^{\,(0)})$. Assuming first just one $n=1$ iteration, the final step (109) becomes

$$\begin{aligned}v' &= v_j^{(0)} + A_j(\vec{v}^{\,(0)})\Delta t + X_j(\vec{v}^{\,(0)})\,\Delta t\\ &\quad+\sum_k \frac{dX_j}{dv_k}(\vec{v}^{\,(0)})\,X_j(\vec{v}^{\,(0)})\frac{(\Delta t)^2}{2} + \mathcal{O}(\Delta t)^{3/2}.\end{aligned} \tag{121}$$

It turns out that iterations of $n>1$ do not affect the expression (121) at $\mathcal{O}(\Delta t)$. The new term in (121) breaks the equivalence of the algorithm (117) because it is of the same order as the drift $A_j\Delta t$.

To restore equivalence, one can add a correction C_j to the drift used in the algorithm as per

$$A_j \to A_j + C_j. \tag{122}$$

in either the "strongly convergent" form

$$C_j^{\rm strong} = -\frac{\Delta t}{2}\sum_k \frac{dX_j}{dv_k}(\vec{v})\, X_j(\vec{v}) \qquad (123)$$

or the "weakly convergent" averaged form $C_j = \left\langle C_j^{\rm strong}\right\rangle_{\rm stoch}$. For the case of Ito-Euler propagator in the midstep algorithm,

$$C_j = C_j^{\rm Strat} = -\frac{\Delta t}{2}\left\langle \sum_k \frac{dX_j}{dv_k}(\vec{v})\, X_j(\vec{v})\right\rangle_{\rm stoch} . \qquad (124)$$

The strong forms (123) have different values for each stochastic realization [51] and obtain $\mathcal{O}(\Delta t)$ timestep accuracy for the noise terms, while the weak forms use a pre-calculated mean (124). The weak variant is more commonly used in practice and sufficient to obtain overall stable and accurate integration. It is what is applied in (114) and the calculations of Sec. 7.

The weak autocorrelation correction C_j has often been dubbed a "Stratonovich correction" because the form (124) is identical to the correction used to move between Ito and Stratonovich stochastic calculus. However, this is a misnomer because the match is merely a coincidence that occurs when an Ito-Euler propagator is used with the midpoint algorithm. For the case of the partly exponential propagator (112), the same procedure as above leads to the following, different, form of the autocorrelation corrections. When $n \geqslant 1$ in the midstep algorithm:

$$C_j = C_j^{\rm Strat} + \frac{\Delta t}{2}\left\langle X_j^E(\vec{v}) X_j^L(\vec{v})\right\rangle_{\rm stoch}, \qquad (125)$$

or when one uses no midstepping ($n = 0$):

$$C_j = -\frac{\Delta t}{2}\left\langle X_j^E(\vec{v}) X_j^E(\vec{v}) v_j + X_j^E(\vec{v}) X_j^R(\vec{v})\right\rangle_{\rm stoch}. \qquad (126)$$

As it happens, in the case of the equations (98), the corrections are the same whether using an Ito-Euler propagator ((114)) or the partially exponential one (125)-(126), but that is not always the case.

A.3 Noise implementation

Since the underlying stochastic equations are defined in the infinitesimal limit $\Delta t \to 0$, in principle any implementation of the noise that has zero mean and satisfies the variance conditions (99) and (100) in the $\Delta t \to 0$ limit is correct. By the central limit theorem, after several timesteps the effective distribution of the sum of the noises will always converge to a Gaussian one. In practice, however, it is usually desirable to use explicitly Gaussian distributed noises in the implementation. Doing so already accurately depicts the limiting distribution for each Δt step and avoids a potential need to reduce timestep further to capture the right noise distribution. For real noises ξ, one generates fresh Gaussian random variables of variance $1/\Delta t$ for each j at the beginning of each timestep. Generating new ones for each time step ensures the $\delta(t-t')$ limit as $\Delta t \to 0$. The Box-Muller algorithm [17] is a simple way to obtain two such independent Gaussian variables from two uniformly distributed noises, whereas a variety of more efficient though less transparent algorithms are also known [12, 18]. In our case Box-Muller was used, while the underlying uniformly distributed noise was generated using the SFMT fast Mersenne twister method [121] [5]. Complex noise η is simply constructed as $\eta = (\xi_r + i\xi_i)/\sqrt{2}$ using two real Gaussian noises $\xi_{i,r}$.

When using efficient random number generation such as [121] it turns out that the creation of Gaussian noises from uniform ones is the most computationally costly step. The Brent algorithm [18] alleviates this appreciably, while a simple alternative route applicable at least for stochastic simulations – due to their central limit properties – is to produce binomially distributed noise instead. One adds n_B uniform noises r_n on $[0,1]$ as per $\xi \approx \sqrt{\frac{12}{n_B \Delta t}}\sum_{n=1}^{n_B}(r_n - \frac{1}{2})$. In practice $n_B = 4$ or $n_B = 3$ is already sufficient.

A.4 Error estimation

Statistical uncertainty in quantities $\mathcal{Q}$ calculated from the simulations can be robustly estimated via subensemble averaging [140] even when the distribution of samples is unknown. The full ensemble of, say $\mathcal{S}$, realisations is divided into a smaller number u of subensembles. Auxiliary subensemble means $\overline{\mathcal{Q}}_{(i=1,\ldots,u)}$ are calculated for each sub-ensemble individually. Then by the central limit theorem, the 1σ uncertainty in the full ensemble prediction is

$$\Delta\mathcal{Q} = \sqrt{\frac{\mathrm{var}\left[\overline{\mathcal{Q}}_{(i)}\right]}{u-1}}. \qquad (127)$$

In practice $u \lesssim \sqrt{\mathcal{S}}$ is useful. In the simulations reported in this paper, $u = 32$ was used.

A separate issue is testing the time discretization accuracy in stochastic equations. In a simple implementation where noise is generated sequentially, changing timestep changes also the noise history, making comparison of single trajectories with different Δt useless for determination of accuracy. Yet, comparing the ensemble means for different timesteps can be onerous in large systems. A solution is to compare two runs of a single realisation with identical underlying noise sources

[5] http://www.math.sci.hiroshima-u.ac.jp/m-mat/MT/SFMT/

[51]: One with time step Δt and noises $\xi_j^{(i)}$ generated sequentially for time steps numbered $i = 1, \ldots$. The other with integration timestep $2\Delta t$ but noises generated by adding pairs of noises from the first simulation: $\xi_j^{(j)\prime} = \xi_j^{(2j-1)} + \xi_j^{(2j)}$. This allows separation of the time discretization error from the stochastic randomness.

References

[1] G. S. Agarwal. Phase-space analysis of time-correlation functions. *Phys. Rev.*, 177:400–407, 1969. DOI: https://doi.org/10.1103/PhysRev.177.400.

[2] G. S. Agarwal. Master equations in phase-space formulation of quantum optics. *Phys. Rev.*, 178:2025–2035, 1969. DOI: https://doi.org/10.1103/PhysRev.178.2025.

[3] G. S. Agarwal and S. Chaturvedi. Scheme to measure the positive P distribution. *Phys. Rev. A*, 49:R665–R667, 1994. DOI: https://doi.org/10.1103/PhysRevA.49.R665.

[4] G. S. Agarwal and E. Wolf. Calculus for functions of noncommuting operators and general phase-space methods in quantum mechanics. II. quantum mechanics in phase space. *Phys. Rev. D*, 2:2187–2205, 1970. DOI: https://doi.org/10.1103/PhysRevD.2.2187.

[5] G. S. Agarwal and E. Wolf. Calculus for functions of noncommuting operators and general phase-space methods in quantum mechanics. III. a generalized Wick theorem and multitime mapping. *Phys. Rev. D*, 2:2206–2225, 1970. DOI: https://doi.org/10.1103/PhysRevD.2.2206.

[6] Takeshi Aimi and Masatoshi Imada. Gaussian-Basis Monte Carlo Method for Numerical Study on Ground States of Itinerant and Strongly Correlated Electron Systems. *J. Phys. Soc. Jpn.*, 76:084709, 2007. DOI: https://doi.org/10.1143/JPSJ.76.084709.

[7] Takeshi Aimi and Masatoshi Imada. Does Simple Two-Dimensional Hubbard Model Account for High-T_c Superconductivity in Copper Oxides? *J. Phys. Soc. Jpn.*, 76:113708, 2007. DOI: https://doi.org/10.1143/JPSJ.76.113708.

[8] Francesco Albarelli, Marco G. Genoni, Matteo G. A. Paris, and Alessandro Ferraro. Resource theory of quantum non-Gaussianity and Wigner negativity. *Phys. Rev. A*, 98:052350, 2018. DOI: https://doi.org/10.1103/PhysRevA.98.052350.

[9] Juan Atalaya, Shay Hacohen-Gourgy, Leigh S. Martin, Irfan Siddiqi, and Alexander N. Korotkov. Multitime correlators in continuous measurement of qubit observables. *Phys. Rev. A*, 97:020104, 2018. DOI: https://doi.org/10.1103/PhysRevA.97.020104.

[10] Motoaki Bamba, Atac Imamoğlu, Iacopo Carusotto, and Cristiano Ciuti. Origin of strong photon antibunching in weakly nonlinear photonic molecules. *Phys. Rev. A*, 83:021802, 2011. DOI: https://doi.org/10.1103/PhysRevA.83.021802.

[11] D. W. Barry and P. D. Drummond. Qubit phase space: SU(n) coherent-state P representations. *Phys. Rev. A*, 78:052108, 2008. DOI: https://doi.org/10.1103/PhysRevA.78.052108.

[12] J. R. Bell. Algorithm 334, normal random deviates. *Communications of the ACM*, 11(7):498, 1968. DOI: https://doi.org/10.1145/363397.363547.

[13] B. Berg, L. I. Plimak, A. Polkovnikov, M. K. Olsen, M. Fleischhauer, and W. P. Schleich. Commuting heisenberg operators as the quantum response problem: Time-normal averages in the truncated Wigner representation. *Phys. Rev. A*, 80:033624, 2009. DOI: https://doi.org/10.1103/PhysRevA.80.033624.

[14] P. B. Blakie, A. S. Bradley, M. J. Davis, R. J. Ballagh, and C. W. Gardiner. Dynamics and statistical mechanics of ultra-cold Bose gases using c-field techniques. *Advances in Physics*, 57(5):363–455, 2008. DOI: https://doi.org/10.1080/00018730802564254.

[15] A. Bohrdt, C. B. Mendl, M. Endres, and M. Knap. Scrambling and thermalization in a diffusive quantum many-body system. *New Journal of Physics*, 19(6):063001, 2017. DOI: https://doi.org/10.1088/1367-2630/aa719b.

[16] Denys I. Bondar, Renan Cabrera, Dmitry V. Zhdanov, and Herschel A. Rabitz. Wigner phase-space distribution as a wave function. *Phys. Rev. A*, 88:052108, 2013. DOI: https://doi.org/10.1103/PhysRevA.88.052108.

[17] G. E. P. Box and Mervin E. Muller. A Note on the Generation of Random Normal Deviates. *The Annals of Mathematical Statistics*, 29(2):610 – 611, 1958. DOI: https://doi.org/10.1214/aoms/1177706645.

[18] Richard P. Brent. Algorithm 488, a Gaussian pseudo-random number generator. *Communications of the ACM*, 17(12):704, 1974. DOI: https://doi.org/10.1145/361604.361629.

[19] K. E. Cahill and R. J. Glauber. Ordered expansions in boson amplitude operators. *Phys. Rev.*, 177:1857–1881, 1969. DOI: https://doi.org/10.1103/PhysRev.177.1857.

[20] K. E. Cahill and R. J. Glauber. Density operators and quasiprobability distribu-

tions. *Phys. Rev.*, 177:1882–1902, 1969. DOI: https://doi.org/10.1103/PhysRev.177.1882.

[21] S. J. Carter, P. D. Drummond, M. D. Reid, and R. M. Shelby. Squeezing of quantum solitons. *Phys. Rev. Lett.*, 58:1841–1844, 1987. DOI: https://doi.org/10.1103/PhysRevLett.58.1841.

[22] I. Carusotto and Y. Castin. An exact stochastic field method for the interacting Bose gas at thermal equilibrium. *Journal of Physics B: Atomic, Molecular and Optical Physics*, 34(23): 4589, 2001. DOI: https://doi.org/10.1088/0953-4075/34/23/305.

[23] Iacopo Carusotto and Yvan Castin. Exact reformulation of the bosonic many-body problem in terms of stochastic wave functions: an elementary derivation. *Ann. Henri Poincaré*, 4(2):783–792, 2003. DOI: https://doi.org/10.1007/s00023-003-0961-7.

[24] W. Casteels, R. Rota, F. Storme, and C. Ciuti. Probing photon correlations in the dark sites of geometrically frustrated cavity lattices. *Phys. Rev. A*, 93:043833, 2016. DOI: https://doi.org/10.1103/PhysRevA.93.043833.

[25] M. Cheneau, P. Barmettler, D. Poletti, M. Endres, P. Schauß, T. Fukuhara, C. Gross, I. Bloch, C. Kollath, and S. Kuhr. Light-cone-like spreading of correlations in a quantum many-body system. *Nature*, 484:484–487, 2012. DOI: https://doi.org/10.1038/nature10748.

[26] Alessio Chiocchetta and Iacopo Carusotto. Quantum langevin model for nonequilibrium condensation. *Phys. Rev. A*, 90:023633, 2014. DOI: https://doi.org/10.1103/PhysRevA.90.023633.

[27] J. F. Corney and P. D. Drummond. Gaussian Quantum Monte Carlo Methods for Fermions and Bosons. *Phys. Rev. Lett.*, 93:260401, 2004. DOI: https://doi.org/10.1103/PhysRevLett.93.260401.

[28] J. F. Corney, P. D. Drummond, and A. Liebman. Quantum noise limits to terabaud communications. *Opt. Commun.*, 140:211–215, 1997. DOI: https://doi.org/10.1016/S0030-4018(97)00191-0.

[29] Joel F. Corney, Peter D. Drummond, Joel Heersink, Vincent Josse, Gerd Leuchs, and Ulrik L. Andersen. Many-body quantum dynamics of polarization squeezing in optical fibers. *Phys. Rev. Lett.*, 97:023606, 2006. DOI: https://doi.org/10.1103/PhysRevLett.97.023606.

[30] Joel F. Corney, Joel Heersink, Ruifang Dong, Vincent Josse, Peter D. Drummond, Gerd Leuchs, and Ulrik L. Andersen. Simulations and experiments on polarization squeezing in optical fiber. *Phys. Rev. A*, 78:023831, 2008. DOI: https://doi.org/10.1103/PhysRevA.78.023831.

[31] Fernando A. M. de Oliveira. s-order nondiagonal quasiprobabilities. *Phys. Rev. A*, 45:5104–5112, 1992. DOI: https://doi.org/10.1103/PhysRevA.45.5104.

[32] K. Dechoum, P. D. Drummond, S. Chaturvedi, and M. D. Reid. Critical fluctuations and entanglement in the nondegenerate parametric oscillator. *Phys. Rev. A*, 70:053807, 2004. DOI: https://doi.org/10.1103/PhysRevA.70.053807.

[33] Graham R. Dennis, Joseph J. Hope, and Mattias T. Johnsson. XMDS2: Fast, scalable simulation of coupled stochastic partial differential equations. *Computer Physics Communications*, 184(1):201–208, 2013. DOI: https://doi.org/10.1016/j.cpc.2012.08.016.

[34] P. Deuar. *First-principles quantum simulations of many-mode open interacting Bose gases using stochastic gauge methods*. PhD thesis, University of Queensland, arXiv:cond-mat/0507023, 2005. URL `https://arxiv.org/abs/cond-mat/0507023`.

[35] P. Deuar. Simulation of complete many-body quantum dynamics using controlled quantum-semiclassical hybrids. *Phys. Rev. Lett.*, 103:130402, 2009. DOI: https://doi.org/10.1103/PhysRevLett.103.130402.

[36] P. Deuar. A tractable prescription for large-scale free flight expansion of wavefunctions. *Computer Physics Communications*, 208:92 – 102, 2016. DOI: http://dx.doi.org/10.1016/j.cpc.2016.08.004.

[37] P. Deuar and P. D. Drummond. Gauge P representations for quantum-dynamical problems: Removal of boundary terms. *Phys. Rev. A*, 66:033812, 2002. DOI: https://doi.org/10.1103/PhysRevA.66.033812.

[38] P. Deuar and P. D. Drummond. First-principles quantum dynamics in interacting Bose gases: I. the positive P representation. *Journal of Physics A: Mathematical and General*, 39(5): 1163, 2006. DOI: https://doi.org/10.1088/0305-4470/39/5/010.

[39] P. Deuar and P. D. Drummond. Correlations in a BEC collision: First-principles quantum dynamics with 150 000 atoms. *Phys. Rev. Lett.*, 98:120402, 2007. DOI: https://doi.org/10.1103/PhysRevLett.98.120402.

[40] P. Deuar, A. G. Sykes, D. M. Gangardt, M. J. Davis, P. D. Drummond, and K. V. Kheruntsyan. Nonlocal pair correlations in the one-dimensional Bose gas at finite temperature. *Phys. Rev. A*, 79:043619, 2009. DOI: https://doi.org/10.1103/PhysRevA.79.043619.

[41] P. Deuar, J. Chwedeńczuk, M. Trippenbach, and P. Ziń. Bogoliubov dynamics of conden-

sate collisions using the positive-P representation. *Phys. Rev. A*, 83:063625, 2011. DOI: https://doi.org/10.1103/PhysRevA.83.063625.

[42] P. Deuar, T. Wasak, P. Ziń, J. Chwedeńczuk, and M. Trippenbach. Tradeoffs for number squeezing in collisions of Bose-Einstein condensates. *Phys. Rev. A*, 88:013617, 2013. DOI: https://doi.org/10.1103/PhysRevA.88.013617.

[43] P. Deuar, J.-C. Jaskula, M. Bonneau, V. Krachmalnicoff, D. Boiron, C. I. Westbrook, and K. V. Kheruntsyan. Anisotropy in s-wave Bose-Einstein condensate collisions and its relationship to superradiance. *Phys. Rev. A*, 90:033613, 2014. DOI: https://doi.org/10.1103/PhysRevA.90.033613.

[44] Piotr Deuar and Joanna Pietraszewicz. A semiclassical field theory that is freed of the ultraviolet catastrophe, 2019. URL `https://arxiv.org/abs/1904.06266`. arXiv:1904.06266.

[45] Piotr Deuar, Alex Ferrier, Michał Matuszewski, Giuliano Orso, and Marzena H. Szymańska. Fully quantum scalable description of driven-dissipative lattice models. *PRX Quantum*, 2:010319, 2021. DOI: https://doi.org/10.1103/PRXQuantum.2.010319.

[46] Mark R. Dowling, Peter D. Drummond, Matthew J. Davis, and Piotr Deuar. Time-reversal test for stochastic quantum dynamics. *Phys. Rev. Lett.*, 94:130401, 2005. DOI: https://doi.org/10.1103/PhysRevLett.94.130401.

[47] P. D. Drummond. Central partial difference propagation algorithms. *Computer Physics Communications*, 29(3):211–225, 1983. DOI: https://doi.org/10.1016/0010-4655(83)90001-2.

[48] P. D. Drummond. Fundamentals of higher order stochastic equations. *J. Phys. A*, 47(33):335001, 2014. DOI: https://doi.org/10.1088/1751-8113/47/33/335001.

[49] P. D. Drummond and J. F. Corney. Quantum dynamics of evaporatively cooled Bose-Einstein condensates. *Phys. Rev. A*, 60:R2661–R2664, 1999. DOI: https://doi.org/10.1103/PhysRevA.60.R2661.

[50] P. D. Drummond and C. W. Gardiner. Generalised P-representations in quantum optics. *Journal of Physics A: Mathematical and General*, 13(7):2353, 1980. DOI: https://doi.org/10.1088/0305-4470/13/7/018.

[51] P. D. Drummond and I. K. Mortimer. Computer simulations of multiplicative stochastic differential equations. *Journal of Computational Physics*, 93(1):144–170, 1991. DOI: https://doi.org/10.1016/0021-9991(91)90077-X.

[52] P. D. Drummond and D. F. Walls. Quantum theory of optical bistability. I. nonlinear polarisability model. *Journal of Physics A: Mathematical and General*, 13(2):725–741, 1980. DOI: https://doi.org/10.1088/0305-4470/13/2/034.

[53] P. D. Drummond, B. Opanchuk, L. Rosales-Zárate, M. D. Reid, and P. J. Forrester. Scaling of boson sampling experiments. *Phys. Rev. A*, 94:042339, 2016. DOI: https://doi.org/10.1103/PhysRevA.94.042339.

[54] Peter D. Drummond and Bogdan Opanchuk. Initial states for quantum field simulations in phase space. *Phys. Rev. Research*, 2:033304, 2020. DOI: https://doi.org/10.1103/PhysRevResearch.2.033304.

[55] Dominic V. Else, Bela Bauer, and Chetan Nayak. Floquet time crystals. *Phys. Rev. Lett.*, 117:090402, 2016. DOI: https://doi.org/10.1103/PhysRevLett.117.090402.

[56] Ruihua Fan, Pengfei Zhang, Huitao Shen, and Hui Zhai. Out-of-time-order correlation for many-body localization. *Science Bulletin*, 62(10):707–711, 2017. DOI: https://doi.org/10.1016/j.scib.2017.04.011.

[57] M. D. Feit, J. A. Fleck, and A. Steiger. Solution of the Schrödinger equation by a spectral method. *Journal of Computational Physics*, 47(3):412–433, 1982. DOI: http://dx.doi.org/10.1016/0021-9991(82)90091-2.

[58] Christopher Ferrie. Quasi-probability representations of quantum theory with applications to quantum information science. *Reports on Progress in Physics*, 74(11):116001, 2011. DOI: https://doi.org/10.1088/0034-4885/74/11/116001.

[59] S. Finazzi, A. Le Boité, F. Storme, A. Baksic, and C. Ciuti. Corner-space renormalization method for driven-dissipative two-dimensional correlated systems. *Phys. Rev. Lett.*, 115:080604, 2015. DOI: https://doi.org/10.1103/PhysRevLett.115.080604.

[60] Laura Foini and Jorge Kurchan. Eigenstate thermalization hypothesis and out of time order correlators. *Phys. Rev. E*, 99:042139, 2019. DOI: https://doi.org/10.1103/PhysRevE.99.042139.

[61] Matteo Frigo and Steven G. Johnson. The design and implementation of FFTW3. *Proceedings of the IEEE*, 93(2):216–231, 2005. DOI: https://doi.org/10.1109/JPROC.2004.840301.

[62] C. W. Gardiner. *Quantum Noise*. Springer-Verlag, Berlin, 1991. ISBN 9783662096444, 9783662096420.

[63] Martin Gärttner, Justin G. Bohnet, Arghavan Safavi-Naini, Michael L. Wall, John J. Bollinger, and Ana Maria Rey. Measuring out-of-time-order correlations and multiple quantum spectra in a trapped-ion quantum mag-

net. *Nature Physics*, 13(8):781–786, 2017. DOI: https://doi.org/10.1038/nphys4119.

[64] Martin Gärttner, Philipp Hauke, and Ana Maria Rey. Relating out-of-time-order correlations to entanglement via multiple-quantum coherences. *Phys. Rev. Lett.*, 120:040402, 2018. DOI: https://doi.org/10.1103/PhysRevLett.120.040402.

[65] C. Gehrke, J. Sperling, and W. Vogel. Quantification of nonclassicality. *Phys. Rev. A*, 86:052118, 2012. DOI: https://doi.org/10.1103/PhysRevA.86.052118.

[66] A. Gilchrist, C. W. Gardiner, and P. D. Drummond. Positive P representation: Application and validity. *Phys. Rev. A*, 55:3014–3032, 1997. DOI: https://doi.org/10.1103/PhysRevA.55.3014.

[67] Roy J. Glauber. Coherent and incoherent states of the radiation field. *Phys. Rev.*, 131:2766–2788, 1963. DOI: https://doi.org/10.1103/PhysRev.131.2766.

[68] Roy J. Glauber. The quantum theory of optical coherence. *Phys. Rev.*, 130:2529–2539, 1963. DOI: https://doi.org/10.1103/PhysRev.130.2529.

[69] V. Goblot, B. Rauer, F. Vicentini, A. Le Boité, E. Galopin, A. Lemaître, L. Le Gratiet, A. Harouri, I. Sagnes, S. Ravets, C. Ciuti, A. Amo, and J. Bloch. Nonlinear polariton fluids in a flatband reveal discrete gap solitons. *Phys. Rev. Lett.*, 123:113901, 2019. DOI: https://doi.org/10.1103/PhysRevLett.123.113901.

[70] Rong-Qiang He and Zhong-Yi Lu. Characterizing many-body localization by out-of-time-ordered correlation. *Phys. Rev. B*, 95:054201, 2017. DOI: https://doi.org/10.1103/PhysRevB.95.054201.

[71] Scott E. Hoffmann, Joel F. Corney, and Peter D. Drummond. Hybrid phase-space simulation method for interacting Bose fields. *Phys. Rev. A*, 78:013622, 2008. DOI: https://doi.org/10.1103/PhysRevA.78.013622.

[72] A. A. Houck, H. E. Türeci, and J. Koch. On-chip quantum simulation with superconducting circuits. *Nature Physics*, 8:292–299, 2012. DOI: https://doi.org/10.1038/nphys2251.

[73] Julian Huber, Peter Kirton, and Peter Rabl. Phase-Space Methods for Simulating the Dissipative Many-Body Dynamics of Collective Spin Systems. *SciPost Phys.*, 10:45, 2021. URL https://scipost.org/10.21468/SciPostPhys.10.2.045.

[74] M. R. Hush, S. S. Szigeti, A. R. R. Carvalho, and J. J. Hope. Controlling spontaneous-emission noise in measurement-based feedback cooling of a Bose-Einstein condensate. *New J. Phys.*, 15(11):113060, 2013. DOI: https://doi.org/10.1088/1367-2630/15/11/113060.

[75] K. Husimi. Some formal properties of the density matrix. *Proc. Phys. Math. Soc. Jpn.*, 22:264–314, 1940. DOI: https://doi.org/10.11429/ppmsj1919.22.4_264.

[76] Nobuyuki Ikeda and Shinzo Watanabe. *Stochastic Differential Equations and Diffusion Processes*, volume 24 of *North-Holland Mathematical Library*. North Holland, 2nd edition, 1988. ISBN 0444861726, 9780444861726.

[77] Juha Javanainen and Janne Ruostekoski. Symbolic calculation in development of algorithms: split-step methods for the Gross–Pitaevskii equation. *Journal of Physics A: Mathematical and General*, 39(12):L179, 2006. DOI: https://doi.org/10.1088/0305-4470/39/12/L02.

[78] Kai Ji, Vladimir N. Gladilin, and Michiel Wouters. Temporal coherence of one-dimensional nonequilibrium quantum fluids. *Phys. Rev. B*, 91:045301, 2015. DOI: https://doi.org/10.1103/PhysRevB.91.045301.

[79] Guy Jumarie. Complex-valued Wiener measure: An approach via random walk in the complex plane. *Statistics and Probability Letters*, 42(1):61–67, 1999. DOI: https://doi.org/10.1016/S0167-7152(98)00194-1.

[80] Guy Jumarie. On the representation of fractional brownian motion as an integral with respect to $(dt)^a$. *Applied Mathematics Letters*, 18(7):739–748, 2005. DOI: https://doi.org/10.1016/j.aml.2004.05.014.

[81] P. L. Kelley and W. H. Kleiner. Theory of electromagnetic field measurement and photoelectron counting. *Phys. Rev.*, 136:A316–A334, 1964. DOI: https://doi.org/10.1103/PhysRev.136.A316.

[82] K. V. Kheruntsyan, J.-C. Jaskula, P. Deuar, M. Bonneau, G. B. Partridge, J. Ruaudel, R. Lopes, D. Boiron, and C. I. Westbrook. Violation of the Cauchy-Schwarz inequality with matter waves. *Phys. Rev. Lett.*, 108:260401, 2012. DOI: https://doi.org/10.1103/PhysRevLett.108.260401.

[83] T. Kiesel, W. Vogel, V. Parigi, A. Zavatta, and M. Bellini. Experimental determination of a nonclassical Glauber-Sudarshan P function. *Phys. Rev. A*, 78:021804, 2008. DOI: https://doi.org/10.1103/PhysRevA.78.021804.

[84] S. Kiesewetter, Q. Y. He, P. D. Drummond, and M. D. Reid. Scalable quantum simulation of pulsed entanglement and Einstein-Podolsky-Rosen steering in optomechanics. *Phys. Rev. A*, 90:043805, 2014. DOI: https://doi.org/10.1103/PhysRevA.90.043805.

[85] P. Kinsler and P. D. Drummond. Quantum dynamics of the parametric oscillator. *Phys. Rev. A*, 43:6194–6208, 1991. DOI: https://doi.org/10.1103/PhysRevA.43.6194.

[86] Katja Klobas, Matthieu Vanicat, Juan P Garrahan, and Tomaž Prosen. Matrix product state of multi-time correlations. *Journal of Physics A: Mathematical and Theoretical*, 53(33):335001, 2020. DOI: https://doi.org/10.1088/1751-8121/ab8c62.

[87] Peter E. Kloeden and Eckhard Platen. *Numerical solution of stochastic differential equations*. Stochastic Modelling and Applied Probability. Springer-verlag, Berlin Heidelberg, 1992. ISBN 978-3-540-54062-5. DOI: https://doi.org/10.1007/978-3-662-12616-5.

[88] J. K. Korbicz, J. I. Cirac, Jan Wehr, and M. Lewenstein. Hilbert's 17th problem and the quantumness of states. *Phys. Rev. Lett.*, 94:153601, 2005. DOI: https://doi.org/10.1103/PhysRevLett.94.153601.

[89] F. Krumm, J. Sperling, and W. Vogel. Multitime correlation functions in nonclassical stochastic processes. *Phys. Rev. A*, 93:063843, 2016. DOI: https://doi.org/10.1103/PhysRevA.93.063843.

[90] Ryogo Kubo, Morikazu Toda, and Natsuki Hashitsume. *Statistical Physics II*. Springer-Verlag, Berlin, 1985. ISBN 978-3-540-53833-2. DOI: https://doi.org/10.1007/978-3-642-58244-8.

[91] C. Lamprecht, M. K. Olsen, P. D. Drummond, and H. Ritsch. Positive-P and Wigner representations for quantum-optical systems with nonorthogonal modes. *Phys. Rev. A*, 65:053813, 2002. DOI: https://doi.org/10.1103/PhysRevA.65.053813.

[92] Melvin Lax. Quantum noise. XI. multitime correspondence between quantum and classical stochastic processes. *Phys. Rev.*, 172:350–361, 1968. DOI: https://doi.org/10.1103/PhysRev.172.350.

[93] Hai-Woong Lee. Theory and application of the quantum phase-space distribution functions. *Physics Reports*, 259(3):147–211, 1995. DOI: https://doi.org/10.1016/0370-1573(95)00007-4.

[94] R. J. Lewis-Swan and K. V. Kheruntsyan. Proposal for demonstrating the Hong–Ou–Mandel effect with matter waves. *Nature Commun.*, 5:3752, 2014. DOI: https://doi.org/10.1038/ncomms4752.

[95] R. J. Lewis-Swan and K. V. Kheruntsyan. Proposal for a motional-state Bell inequality test with ultracold atoms. *Phys. Rev. A*, 91:052114, 2015. DOI: https://doi.org/10.1103/PhysRevA.91.052114.

[96] T. C. H. Liew and V. Savona. Single photons from coupled quantum modes. *Phys. Rev. Lett.*, 104:183601, 2010. DOI: https://doi.org/10.1103/PhysRevLett.104.183601.

[97] Andreas M Läuchli and Corinna Kollath. Spreading of correlations and entanglement after a quench in the one-dimensional Bose-Hubbard model. *Journal of Statistical Mechanics: Theory and Experiment*, 2008(05):P05018, 2008. DOI: https://doi.org/10.1088/1742-5468/2008/05/p05018.

[98] Juan Maldacena, Stephen H. Shenker, and Douglas Stanford. A bound on chaos. *Journal of High Energy Physics*, 2016(8):106, 2016. DOI: https://doi.org/10.1007/JHEP08(2016)106.

[99] L. Mandel. Antinormally ordered correlations and quantum counters. *Phys. Rev.*, 152:438–451, 1966. DOI: https://doi.org/10.1103/PhysRev.152.438.

[100] Stephan Mandt, Darius Sadri, Andrew A Houck, and Hakan E Türeci. Stochastic differential equations for quantum dynamics of spin-boson networks. *New Journal of Physics*, 17(5):053018, 2015. DOI: https://doi.org/10.1088/1367-2630/17/5/053018.

[101] Amy C. Mathey, Charles W. Clark, and L. Mathey. Decay of a superfluid current of ultracold atoms in a toroidal trap. *Phys. Rev. A*, 90:023604, 2014. DOI: https://doi.org/10.1103/PhysRevA.90.023604.

[102] S. L. W. Midgley, S. Wüster, M. K. Olsen, M. J. Davis, and K. V. Kheruntsyan. Comparative study of dynamical simulation methods for the dissociation of molecular Bose-Einstein condensates. *Phys. Rev. A*, 79:053632, 2009. DOI: https://doi.org/10.1103/PhysRevA.79.053632.

[103] Magdalena Moczała-Dusanowska, Łukasz Dusanowski, Stefan Gerhardt, Yu Ming He, Marcus Reindl, Armando Rastelli, Rinaldo Trotta, Niels Gregersen, Sven Höfling, and Christian Schneider. Strain-tunable single-photon source based on a quantum dot–micropillar system. *ACS Photonics*, 6(8):2025–2031, 2019. DOI: https://doi.org/10.1021/acsphotonics.9b00481.

[104] Ekaterina Moreva, Marco Gramegna, Giorgio Brida, Lorenzo Maccone, and Marco Genovese. Quantum time: Experimental multitime correlations. *Phys. Rev. D*, 96:102005, 2017. DOI: https://doi.org/10.1103/PhysRevD.96.102005.

[105] J. E. Moyal. Quantum mechanics as a statistical theory. *Mathematical Proceedings of the Cambridge Philosophical Society*, 45(01):99–124, 1949. DOI: https://doi.org/10.1017/S0305004100000487.

[106] Ray Ng and Erik S. Sørensen. Exact real-time

dynamics of quantum spin systems using the positive-P representation. *J. Phys. A*, 44:065305, 2011. DOI: https://doi.org/10.1088/1751-8113/44/6/065305.

[107] Ray Ng, Erik S. Sørensen, and Piotr Deuar. Simulation of the dynamics of many-body quantum spin systems using phase-space techniques. *Phys. Rev. B*, 88:144304, 2013. DOI: https://doi.org/10.1103/PhysRevB.88.144304.

[108] A. A. Norrie, R. J. Ballagh, and C. W. Gardiner. Quantum turbulence in condensate collisions: An application of the classical field method. *Phys. Rev. Lett.*, 94:040401, 2005. DOI: https://doi.org/10.1103/PhysRevLett.94.040401.

[109] M. K. Olsen, L. I. Plimak, and M. Fleischhauer. Quantum-theoretical treatments of three-photon processes. *Phys. Rev. A*, 65:053806, 2002. DOI: https://doi.org/10.1103/PhysRevA.65.053806.

[110] M. K. Olsen, A. B. Melo, K. Dechoum, and A. Z. Khoury. Quantum phase-space analysis of the pendular cavity. *Phys. Rev. A*, 70:043815, 2004. DOI: https://doi.org/10.1103/PhysRevA.70.043815.

[111] Bogdan Opanchuk, Rodney Polkinghorne, Oleksandr Fialko, Joachim Brand, and Peter D. Drummond. Quantum simulations of the early universe. *Annalen der Physik*, 525(10-11):866–876, 2013. DOI: https://doi.org/10.1002/andp.201300113.

[112] Bogdan Opanchuk, Laura Rosales-Zárate, Margaret D. Reid, and Peter D. Drummond. Simulating and assessing boson sampling experiments with phase-space representations. *Phys. Rev. A*, 97:042304, 2018. DOI: https://doi.org/10.1103/PhysRevA.97.042304.

[113] Bogdan Opanchuk, Laura Rosales-Zárate, Margaret D. Reid, and Peter D. Drummond. Robustness of quantum Fourier transform interferometry. *Opt. Lett.*, 44(2):343–346, 2019. DOI: https://doi.org/10.1364/OL.44.000343.

[114] J. Pietraszewicz, M. Stobińska, and P. Deuar. Correlation evolution in dilute Bose-Einstein condensates after quantum quenches. *Phys. Rev. A*, 99:023620, 2019. DOI: https://doi.org/10.1103/PhysRevA.99.023620.

[115] L. I. Plimak and M. K. Olsen. Quantum-field-theoretical approach to phase–space techniques: Symmetric Wick theorem and multitime Wigner representation. *Annals of Physics*, 351:593 – 619, 2014. DOI: https://doi.org/10.1016/j.aop.2014.09.010.

[116] L. I. Plimak, M. K. Olsen, M. Fleischhauer, and M. J. Collett. Beyond the Fokker-Planck equation: Stochastic simulation of complete Wigner representation for the optical parametric oscillator. *Europhysics Letters (EPL)*, 56(3):372–378, 2001. DOI: https://doi.org/10.1209/epl/i2001-00529-8.

[117] L. I. Plimak, M. Fleischhauer, M. K. Olsen, and M. J. Collett. Quantum-field-theoretical approach to phase-space techniques: Generalizing the positive-P representation. *Phys. Rev. A*, 67:013812, 2003. DOI: https://doi.org/10.1103/PhysRevA.67.013812.

[118] Anatoli Polkovnikov. Phase space representation of quantum dynamics. *Annals of Physics*, 325(8):1790 – 1852, 2010. DOI: http://dx.doi.org/10.1016/j.aop.2010.02.006.

[119] Martin Ringbauer, Fabio Costa, Michael E. Goggin, Andrew G. White, and Fedrizzi Alessandro. Multi-time quantum correlations with no spatial analog. *NPJ Quantum Information*, 4:37, 2018. DOI: https://doi.org/10.1038/s41534-018-0086-y.

[120] J. A. Ross, P. Deuar, D. K. Shin, K. F. Thomas, B. M. Henson, S. S. Hodgman, and A. G Truscott. Survival of the quantum depletion of a condensate after release from a harmonic trap in theory and experiment, 2021. URL `https://arxiv.org/abs/2103.15283`. arXiv:2103.15283.

[121] Mutsuo Saito and Makoto Matsumoto. Simd-oriented fast Mersenne twister: a 128-bit pseudorandom number generator. In Alexander Keller, Stefan Heinrich, and Harald Niederreiter, editors, *Monte Carlo and Quasi-Monte Carlo Methods 2006*, pages 607–622, Berlin, Heidelberg, 2008. Springer Berlin Heidelberg. ISBN 978-3-540-74496-2. DOI: https://doi.org/10.1007/978-3-540-74496-2_36.

[122] Sebastian Schmidt and Jens Koch. Circuit qed lattices: Towards quantum simulation with superconducting circuits. *Annalen der Physik*, 525(6):395–412, 2013. DOI: https://doi.org/10.1002/andp.201200261.

[123] C. Schneider, K. Winkler, M. D. Fraser, M. Kamp, Y. Yamamoto, E. A. Ostrovskaya, and S. Höfling. Exciton-polariton trapping and potential landscape engineering. *Reports on Progress in Physics*, 80(1):016503, 2016. DOI: https://doi.org/10.1088/0034-4885/80/1/016503.

[124] Huitao Shen, Pengfei Zhang, Ruihua Fan, and Hui Zhai. Out-of-time-order correlation at a quantum phase transition. *Phys. Rev. B*, 96:054503, 2017. DOI: https://doi.org/10.1103/PhysRevB.96.054503.

[125] Alice Sinatra, Carlos Lobo, and Yvan Castin. The truncated Wigner method for Bose-condensed gases: limits of validity and applications. *Journal of Physics B: Atomic, Molecular and*

Optical Physics, 35(17):3599, 2002. DOI: https://doi.org/10.1088/0953-4075/35/17/301.

[126] A. M. Smith and C. W. Gardiner. Simulations of nonlinear quantum damping using the positive P representation. *Phys. Rev. A*, 39:3511–3524, 1989. DOI: https://doi.org/10.1103/PhysRevA.39.3511.

[127] Robert W. Spekkens. Negativity and contextuality are equivalent notions of nonclassicality. *Phys. Rev. Lett.*, 101:020401, 2008. DOI: https://doi.org/10.1103/PhysRevLett.101.020401.

[128] J. Sperling. Characterizing maximally singular phase-space distributions. *Phys. Rev. A*, 94:013814, 2016. DOI: https://doi.org/10.1103/PhysRevA.94.013814.

[129] J Sperling and W Vogel. Quasiprobability distributions for quantum-optical coherence and beyond. *Physica Scripta*, 95(3):034007, 2020. DOI: https://doi.org/10.1088/1402-4896/ab5501.

[130] Herbert Spohn. Kinetic equations from hamiltonian dynamics: Markovian limits. *Rev. Mod. Phys.*, 52:569–615, 1980. DOI: https://doi.org/10.1103/RevModPhys.52.569.

[131] M. J. Steel, M. K. Olsen, L. I. Plimak, P. D. Drummond, S. M. Tan, M. J. Collett, D. F. Walls, and R. Graham. Dynamical quantum noise in trapped Bose-Einstein condensates. *Phys. Rev. A*, 58:4824–4835, 1998. DOI: https://doi.org/10.1103/PhysRevA.58.4824.

[132] E. C. G. Sudarshan. Equivalence of Semiclassical and Quantum Mechanical Descriptions of Statistical Light Beams. *Phys. Rev. Lett.*, 10:277–279, 1963. DOI: https://doi.org/10.1103/PhysRevLett.10.277.

[133] Brian Swingle, Gregory Bentsen, Monika Schleier-Smith, and Patrick Hayden. Measuring the scrambling of quantum information. *Phys. Rev. A*, 94:040302, 2016. DOI: https://doi.org/10.1103/PhysRevA.94.040302.

[134] Tomasz Świsłocki and Piotr Deuar. Quantum fluctuation effects on the quench dynamics of thermal quasicondensates. *Journal of Physics B: Atomic, Molecular and Optical Physics*, 49(14):145303, 2016. DOI: https://doi.org/10.1088/0953-4075/49/14/145303.

[135] Andrzej Syrwid, Jakub Zakrzewski, and Krzysztof Sacha. Time crystal behavior of excited eigenstates. *Phys. Rev. Lett.*, 119:250602, 2017. DOI: https://doi.org/10.1103/PhysRevLett.119.250602.

[136] Kishore Thapliyal, Subhashish Banerjee, Anirban Pathak, S. Omkar, and V. Ravishankar. Quasiprobability distributions in open quantum systems: Spin-qubit systems. *Annals of Physics*, 362:261–286, 2015. DOI: https://doi.org/10.1016/j.aop.2015.07.029.

[137] Hidekazu Tsukiji, Hideaki Iida, Teiji Kunihiro, Akira Ohnishi, and Toru T. Takahashi. Entropy production from chaoticity in Yang-Mills field theory with use of the Husimi function. *Phys. Rev. D*, 94:091502, 2016. DOI: https://doi.org/10.1103/PhysRevD.94.091502.

[138] Victor Veitch, Christopher Ferrie, David Gross, and Joseph Emerson. Negative quasiprobability as a resource for quantum computation. *New Journal of Physics*, 14(11):113011, 2012. DOI: https://doi.org/10.1088/1367-2630/14/11/113011.

[139] Werner Vogel. Nonclassical correlation properties of radiation fields. *Phys. Rev. Lett.*, 100:013605, 2008. DOI: https://doi.org/10.1103/PhysRevLett.100.013605.

[140] M. J. Werner and P. D. Drummond. Robust algorithms for solving stochastic partial differential equations. *Journal of Computational Physics*, 132(2):312 – 326, 1997. DOI: https://doi.org/10.1006/jcph.1996.5638.

[141] E. Wigner. On the Quantum Correction For Thermodynamic Equilibrium. *Phys. Rev.*, 40:749–759, 1932. DOI: https://doi.org/10.1103/PhysRev.40.749.

[142] Frank Wilczek. Quantum time crystals. *Phys. Rev. Lett.*, 109:160401, 2012. DOI: https://doi.org/10.1103/PhysRevLett.109.160401.

[143] Michiel Wouters and Vincenzo Savona. Stochastic classical field model for polariton condensates. *Phys. Rev. B*, 79:165302, 2009. DOI: https://doi.org/10.1103/PhysRevB.79.165302.

[144] S. Wüster, J. F. Corney, J. M. Rost, and P. Deuar. Quantum dynamics of long-range interacting systems using the positive-P and gauge-P representations. *Phys. Rev. E*, 96:013309, 2017. DOI: https://doi.org/10.1103/PhysRevE.96.013309.

[145] J. Zhang, P. W. Hess, A. Kyprianidis, P. Becker, A. Lee, J. Smith, G. Pagano, I. D. Potirniche, A. C. Potter, A. Vishwanath, N. Y. Yao, and C. Monroe. Observation of a discrete time crystal. *Nature*, 543(7644):217, 2017. DOI: https://doi.org/10.1038/nature21413.